Title

Unique Features of Human Protein Arginine Methyltransferase 9 (PRMT9) and Its Substrate RNA Splicing Factor SF3B2*

Journal

Journal of Biological Chemistry, 290(27)

ISSN

0021-9258

Authors

Hadjikyriacou, Andrea
Yang, Yanzhong
Espejo, Alexsandra
et al.

Publication Date

2015-07-01

DOI

10.1074/jbc.m115.659433

Peer reviewed

THE JOURNAL OF BIOLOGICAL CHEMISTRY VOL. 290, NO. 27, pp. 16723–16743, July 3, 2015

Unique Features of Human Protein Arginine Methyltransferase 9 (PRMT9) and Its Substrate RNA Splicing Factor SF3B2*

Received for publication, April 17, 2015, and in revised form, May 14, 2015 Published, JBC Papers in Press, May 15, 2015, DOI 10.1074/jbc.M115.659433

Andrea Hadjikyriacou[‡], **Yanzhong Yang**[§1], **Alexsandra Espejo**[§], **Mark T. Bedford**[§], and **Steven G. Clarke**[‡2]

From the [‡]*Department of Chemistry and Biochemistry and the Molecular Biology Institute, UCLA, Los, Angeles, California 90095 and the* [§]*Department of Epigenetics and Molecular Carcinogenesis, University of Texas MD Anderson Cancer Center, Smithville, Texas 78957*

Background: Newly discovered protein arginine methyltransferase 9 (PRMT9) modulates alternative splicing by methylation of SF3B2.
Results: Biochemical probes of PRMT9 and its substrate protein revealed domains and residues required for methylation.
Conclusion: PRMT9 is unique among PRMTs in its narrow range of methyl-accepting substrates.
Significance: Understanding PRMT9 catalysis will help elucidate how it may control the activity of SF3B2 and other potential endogenous substrates.

Human protein arginine methyltransferase (PRMT) 9 symmetrically dimethylates arginine residues on splicing factor SF3B2 (SAP145) and has been functionally linked to the regulation of alternative splicing of pre-mRNA. Site-directed mutagenesis studies on this enzyme and its substrate had revealed essential unique residues in the double E loop and the importance of the C-terminal duplicated methyltransferase domain. In contrast to what had been observed with other PRMTs and their physiological substrates, a peptide containing the methylatable Arg-508 of SF3B2 was not recognized by PRMT9 *in vitro*. Although amino acid substitutions of residues surrounding Arg-508 had no great effect on PRMT9 recognition of SF3B2, moving the arginine residue within this sequence abolished methylation. PRMT9 and PRMT5 are the only known mammalian enzymes capable of forming symmetric dimethylarginine (SDMA) residues as type II PRMTs. We demonstrate here that the specificity of these enzymes for their substrates is distinct and not redundant. The loss of PRMT5 activity in mouse embryo fibroblasts results in almost complete loss of SDMA, suggesting that PRMT5 is the primary SDMA-forming enzyme in these cells. PRMT9, with its duplicated methyltransferase domain and conserved sequence in the double E loop, appears to have a unique structure and specificity among PRMTs for methylating SF3B2 and potentially other polypeptides.

Protein arginine methylation is an important post-translational modification in eukaryotic cells catalyzed by the family of PRMTs[3] (1–4). Each member of this family contains a conserved core methyltransferase domain, consisting of *S*-adenosyl-L-methionine (AdoMet)-binding sequences in motif I and post-motif I, and substrate-binding sequences in motif II, post-motif II (including the double E loop), and the THW loop (1–5). The mammalian family of PRMTs has been divided into three groups based on their activities. Type I PRMTs (PRMT1–4, PRMT6, and PRMT8) transfer up to two methyl groups on the same terminal guanidino nitrogen of arginine to form ω-N^G-monomethylarginine (MMA) and ω-N^G,N^G-asymmetric dimethylarginine (ADMA) residues. Type II PRMTs (PRMT5 and PRMT9) transfer methyl groups on different terminal guanidino nitrogen atoms to form MMA and ω-N^G,N'^G-symmetric dimethylarginine (SDMA) residues. Finally, type III enzymes transfer only a single methyl group to form MMA residues (PRMT7) (1–8). Both histone and non-histone proteins have been identified as PRMT substrates (2, 4–6, 9), indicating very diverse and important roles for these arginine-modifying enzymes. For example, dysregulation of PRMT1, the major asymmetric dimethylating enzyme, results in a variety of cancers, including breast, colon, bladder, lung, and various leukemias (5, 10, 11). Overexpression of other PRMTs (2–8) has also been linked to cancer development (particularly breast cancer) through increased cellular proliferation, conferred resistance to DNA-damaging agents, and increased cell invasion (3, 5). The mammalian PRMTs have important roles in transcriptional regulation, signal transduction, nuclear/cytoplasmic shuttling, DNA repair, mRNA splicing, and male germ line gene imprinting (2, 3).

Although most of the mammalian arginine methyltransferases have been extensively studied, the catalytic activity of PRMT9 was unknown until our recent work identified it as the second SDMA-forming enzyme in mammals (7). This enzyme

* This work was supported, in whole or in part, by National Institutes of Health Grants GM026020 (to S. G. C.), DK062248 (to M. T. B.), and GM007185, a Ruth L. Kirschstein National Research Service Award (to A. H.). The authors declare that they have no conflicts of interest with the contents of this article.
[1] Present address: Dept. of Radiation Biology, Beckman Research Institute, City of Hope Cancer Center, Duarte, CA 91010.
[2] To whom correspondence should be addressed: Dept. of Chemistry and Biochemistry and the Molecular Biology Institute, UCLA, 607 Charles E. Young Dr. E., Los Angeles, CA 90095-1569. Tel.: 310-825-8754; Fax: 310-825-1968; E-mail: clarke@mbi.ucla.edu.
[3] The abbreviations used are: PRMT, protein arginine methyltransferase; MMA, ω-N^G-monomethylarginine; ADMA, ω-N^G,N^G-asymmetric dimethylarginine; SDMA, ω-N^G,N'^G-symmetric dimethylarginine; AdoMet, *S*-adenosyl-L-methionine; [*methyl*-^{3}H]AdoMet, *S*-adenosyl-L-[*methyl*-^{3}H]methionine; GAR, glycine- and arginine-rich domain of human fibrillarin; MBP, myelin basic protein; OHT, 4-hydroxytamoxifen; OPA, *o*-phthalaldehyde; MEF, mouse embryo fibroblast; ΔTPR, GST-PRMT9 mutant missing residues 21–139; ΔN, GST-PRMT9 mutant missing residues 21–350; ΔC 529, GST-PRMT9 mutant missing residues 530–895; ΔC 350, mutant missing residues 351–895; Bistris, 2-[bis(2-hydroxyethyl)amino]-2-(hydroxymethyl)propane-1,3-diol.

should be distinguished from the FBXO11 gene product, previously erroneously termed PRMT9, that is a component of an E3 ubiquitin ligase complex (7, 12). Biological assays showed that PRMT9 levels are functionally linked to the regulation of alternative splicing, and PRMT9 was thus identified as a modulator of small nuclear ribonucleoprotein maturation (7). PRMT9 is found in a cellular complex with the splicing factors SF3B2 and SF3B4, also known as SAP145 and SAP49, respectively (7). PRMT9 catalyzes the formation of MMA and SDMA in SF3B2 but had little or no activity on the common *in vitro* substrates of other PRMTs, such as polypeptides with glycine-arginine rich repeats (GAR) (7).

Splicing factor SF3B2 is highly conserved in nature, binds SF3B4 in a tight complex (13, 14), and has implied functional roles in cell cycle progression (14). Previous studies have shown that the HIV accessory protein Vpr interferes with the SF3B2-SF3B4 complex as a mechanism to induce G_2 checkpoint arrest and ensure colocalization in nuclear speckles (14). Because PRMT9 methylates SF3B2 within the highly conserved region that mediates its interaction with Vpr, understanding how SF3B2 is recognized and methylated by PRMT9 might provide a potential anti-HIV role for this enzyme.

PRMT9, like PRMT7, contains an ancestrally duplicated methyltransferase domain (7, 8). Other PRMTs contain only one methyltransferase domain, which makes this an unusual feature of these two "outlier" PRMTs. Crystallographic studies elucidating the structure of *Mus musculus* and *Caenorhabditis elegans* PRMT7 show that AdoMet only binds to the N-terminal domain, and the other methyltransferase domain at the C terminus may have a pseudodimer function (15, 16), mimicking the homodimer structure required for activity of other PRMTs upon binding their substrate (PRMT1, PRMT3, and PRMT5, and *Trypanosoma brucei* PRMT7) (15, 17–19). Deletion of either domain in PRMT7 abolishes its activity (20), as do amino acid substitutions in the C-terminal domain (8), consistent with a role in forming pseudodimers that are necessary for correct substrate binding. In addition, our recent work shows that a full-length PRMT9 is necessary for interaction with SF3B2 (7). In this study, we aimed to determine whether N- and C-terminal truncations in PRMT9 retain methylation activity on SF3B2 *in vitro*. In addition, PRMT9 harbors three tetratricopeptide repeats (TPRs), which often mediate protein-protein interactions (21). We thus wanted to elucidate the functional role of this TPR motif and the two methyltransferase domains.

We are also interested in determining how the specificity of PRMT9 is established, in particular what sets it apart from the other much more promiscuous PRMTs. In the substrate-binding double E loop, there are several residues that are present in the type II (PRMT5 and PRMT9) and type III (PRMT7) enzymes that are not found in the type I enzymes. In particular, the presence of acidic residues in the double E loop of PRMT7 has been shown to play a role in the specificity of this enzyme for methylating arginine residues in R*X*R sequences in an overall basic sequence context (8). It is intriguing that PRMT9 has a double E loop sequence similar to PRMT7. We therefore wanted to biochemically characterize this enzyme, probing for the structural features responsible for its type II activity and substrate specificity. We also hoped to use these studies to identify the residues around the methylated arginine in SF3B2 that are critical for its recognition by the methyltransferase.

PRMT5, the only other well characterized symmetrically dimethylating enzyme (4, 22, 23), has been previously reported to play an important role in spliceosomal U small nuclear ribonucleoprotein maturation (24). It is therefore interesting that PRMT9, the only other SDMA-generating enzyme as yet discovered, also modifies a protein involved in RNA splicing. In studies reported here, we have now used immunoblotting and amino acid analyses to examine whether the roles of PRMT5 and PRMT9 are redundant in the cell. Importantly, understanding the contribution of PRMT9 to the global cellular levels of SDMA will determine its contribution to SDMA-mediated biological activities.

Experimental Procedures

Phylogenetic Tree Construction and Sequence Alignments of PRMT9 and SF3B2 Orthologs—A protein BLAST search was performed using *Homo sapiens* PRMT9 (Q6P2P2) and SF3B2 (Q13435) as the query to determine top-ranked orthologs. Protein sequences were aligned using MUSCLE (multiple-sequence comparison by log expectation) in MEGA6 (Molecular Evolutionary Genetics Analysis) software (25). Phylogenetic trees were generated using the neighbor joining method, and evolutionary distances were determined using *p*-distance. Sequence alignments for comparison of important regions within each ortholog were done using Clustal Omega Multiple Sequence Alignment software (26).

Bacterial Protein Expression and Purification—Human *PRMT9* cDNA was subcloned into a pGEX-6p-1 vector (GE Healthcare, catalog no. 28-9546-48), as described previously (7), and expressed as a GST fusion protein in *Escherichia coli* BL21 Star DE3 cells (Invitrogen, catalog no. C601003), resulting in a fusion protein of the *Schistosoma japonicum* GST (Uniprot P08515) with a linker sequence SDLEVLFQGPLGS and residues 1–845 of PRMT9 (UniProt Q6P2P2-1). The DNA of the construct was sequenced on both strands to confirm insertion and protein identity. Cells containing the GST-PRMT9 plasmid were grown in 4 liters of LB broth (Difco, catalog no. 244610) with 100 μg/ml ampicillin (Fisher, catalog no. BP1760) at 37 °C to an OD_{600} of 0.6. Induction was performed at 18 °C with 0.4 mM isopropyl D-thiogalactopyranoside (Gold Bio, catalog no. I2481C25). After a 19-h induction, the cells were harvested at 5000 × *g* at 4 °C and washed two times with phosphate-buffered saline (PBS, 137 mM NaCl, 2.7 mM KCl, 10 mM Na_2HPO_4, 2 mM KH_2PO_4, pH 7.4). Cells were then either frozen at −80 °C until lysis or immediately resuspended in 16 ml of PBS containing 1 mM phenylmethylsulfonyl fluoride (Sigma, catalog no. P7626) and lysed using an Avestin EmulsiFlex-C3 homogenizer for two cycles at 18,000 p.s.i. (Ottawa, Ontario, Canada). After the lysate was centrifuged at 23,000 × *g* for 50 min, the supernatant containing GST-PRMT9 was added to 1 ml of a 50% slurry of glutathione-Sepharose 4B resin (GE Healthcare, catalog no. 17-0756-01) and rotated at 4 °C for 2 h. The resin was then washed with PBS, and the protein was eluted with 2 ml of 30 mM reduced L-glutathione (Sigma, catalog no. G4251) in 50 mM Tris-HCl, 120 mM NaCl, and 5% glycerol, pH 7.5. The GST-SF3B2(401–550) fragment was generated by subcloning human

TABLE 1
Primers for mutagenesis
Fwd is forward and Rev is reverse.

Primer name	Sequence	T_m
		°C
PRMT9		
L182A/D183A/I184A/G185A	Fwd: 5′-TGT TTG GGG TCC AAA AGT GTT GCG GCC GCT GCG GCA GGA ACT GGA ATA CTA AGC-3′	86.7
	Rev: 5′-GCT TAG TAT TCC AGT TCC TGC CGC AGC GGC CGC AAC ACT TTT GGA CCC CAA ACA-3′	
D258G	Fwd: 5′-A GTT GTA ACA GAA ACT GTC GGT GCA GGT TTA TTT GGA GAA G-3′	78.6
	Rev: 5′-C TTC TCC AAA TAA ACC TGC ACC GAC AGT TTC TGT TAC AAC T-3′	
G260E	Fwd: 5′-GTA ACA GAA ACT GTC GAT GCA GAG TTA TTT GGA GAA GGA ATT GTG G-3′	78.5
	Rev: 5′-C CAC AAT TCC TTC TCC AAA TAA CTC TGC ATC GAC AGT TTC TGT TAC-3′	
Δ TPR	Fwd: 5′-CGC TGG GGC AGC CGG CAA TTT TTA TCG TGT TGC-3′	81.6
	Rev: 5′-GCA ACA CGA TAA AAA TTG CCG GCT GCC CCA GCG-3′	
Δ N	Fwd: 5′-GCT GGG GCA GCC GGC CCT TAT ACA ACT GAA A-3′	80.3
	Rev: 5′-TTT CAG TTG TAT AAG GGC CGG CTG CCC CAG C-3′	
Δ C 350	Fwd: 5′-GCT TAT TCT TCT GTA GAT ACT GAA GAA ACA ATT GAA TAG TAG ACA ACT GAA AAG ATG AGT-3′	82.6
	Rev: 5′-ACT CAT CTT TTC AGT TGT CTA CTA TTC AAT TGT TTC TTC AGT ATC TAC AGA AGA ATA AGC-3′	
Δ C 529	Fwd: 5′-TG GAA TCT ACA GAA ATT GCT TTG CTT TAG TAG ATC CCA TAT CAT GAA GGC TTT AAA ATG G-3′	79.6
	Rev: 5′-C CAT TTT AAA GCC TTC ATG ATA TGG GAT CTA CTA AAG CAA AGC AAT TTC TGT AGA TTC CA-3′	
SF3B2		
K507A/K509A	Fwd: 5′-G CCA CGC CAC TGG TGT TTT GCG CGC GCA TAC CTG CAG GGC AAA C-3′	79.4
	Rev: 5′-G TTT GCC CTG CAG GTA TGC GCG CGC AAA ACA CCA GTG GCG TGG C-3′	
K507R/K509R	Fwd: 5′-CCA CGC CAC TGG TGT TTT AGG CGC AGA TAC CTG CAG G-3′	80.0
	Rev: 5′-C CTG CAG GTA TCT GCG CCT AAA ACA CCA GTG GCG TGG-3′	
K507R/R508K/K509R	Fwd: 5′-TGC CTG TGC CAC GCC ACT GGT GTT TTA GGA AGA GAT ACC TGC AGG GCA A-3′	78.4
	Rev: 5′-T TGC CCT GCA GGT ATC TCT TCC TAA AAC ACC AGT GGC GTG GCA CAG GCA-3′	
K507R/R508K	Fwd: 5′-TGT GCC ACG CCA CTG GTG TTT TAG GAA GAA ATA CCT GCA GGG CAA AC-3′	78.7
	Rev: 5′-GT TTG CCC TGC AGG TAT TTC TTC CTA AAA CAC CAG TGG CGT GGC ACA-3′	
F506A/Y510A	Fwd: 5′-GTG CCA CGC CAC TGG TGT GCT AAG CGC AAA GCC CTG CAG GGC AAA-3′	79.5
	Rev: 5′-TTT GCC CTG CAG GGC TTT GCG CTT AGC ACA CCA GTG GCG TGG CAC-3′	

SF3B2 cDNA into the pGEX-6p-1 vector (7). GST-SF3B2 401–550-residue wild type and mutant fragments were purified in a similar manner, but protein was expressed using 0.5 mM isopropyl D-thiogalactopyranoside and induced for 18–20 h, 250 rpm at 18 °C. GST-GAR was purified as described previously (27). Bovine myelin basic protein was purchased from Sigma (M1891, lyophilized powder). Recombinant human histones were purchased from New England Biolabs (histone H2A, catalog no. M2502S; histone H2B, catalog no. M2505S; histone H3.1, catalog no. M2503S; histone H4, catalog no. M2504; Ipswich, MA). Calf thymus histones type IIA-S were purchased from Sigma (catalog no. H7755). Human recombinant FLAG-tagged PRMT5/MEP50 was purchased from BPS Bioscience (catalog no. 51045, lot 140131). A His-tagged human myelin basic protein construct on a pET15b-TEV plasmid was a generous gift from Dr. Douglas Juers from Whitman College; protein expression was performed under similar conditions, and the protein was purified using HisPur Cobalt Resin (Thermo Scientific, catalog no. 89964), with washing in 50 mM phosphate buffer containing 10 mM imidazole, pH 7.0, and elution using a 50 mM phosphate buffer containing 150 mM imidazole, pH 7.0. The protein was dialyzed overnight into PBS to remove residual imidazole. Proteins were quantified using a Lowry assay after precipitation using 10% trichloroacetic acid, using bovine serum albumin as a standard.

Mutagenesis—PRMT9 was mutated to create a catalytically inactive enzyme by introducing quadruple mutations (L182A/D183A/I184A/G185A) in the conserved AdoMet-binding motif I in both the GST-PRMT9 plasmid described above and in the GFP-PRMT9 plasmid described previously (7). Truncation mutants and double E loop mutants were created on the GST-PRMT9 wild type plasmid using the mutagenized primers listed in Table 1. Double E loop mutants consisted of mutating residues Asp-258 to Gly (D258G) and Gly-260 to Glu (G260E). Truncation mutants for GST-PRMT9 were created using mutagenized primers to remove the indicated amino acids from the plasmid as follows: ΔTPR (residues 21–139), ΔN (residues 21–350), ΔC 529 (stop codons were placed upstream of the C-terminal domain, at positions 529 and 530), and ΔC 350 (stop codons were placed upstream of the C-terminal domain at positions 350 and 351). SF3B2 mutants were created on the GST-SF3B2 401–550 fragment wild type plasmid, using mutagenized primers listed in Table 1. Mutants included K507A/K509A (-FARAY-), K507R/K509R (-FRRRY-), K507R/R508K/K509R (-FRKRY-), K507R/R508K (-FRKKY-), and F506A/Y510A (-AKRKA-). The GST mutant constructs were transformed into BL21 DE3 *E. coli* cells for expression as described above. GFP mutant constructs were transfected into HEK293 cells as described below. Mutagenesis was performed with PCRs set up according to the QuikChange XL site-directed mutagenesis kit (Agilent Technologies Inc., catalog no. 200521), using 50 ng of the appropriate wild type plasmid template, 125 ng of each forward and reverse primer as shown in Table 1, and 1 μl of PfuUltra HF DNA polymerase (2.5 units/μl). The PCR was run at 95 °C for 1 min, 18 cycles of 95 °C for 50 s, 60 °C for 50 s, and 65 °C for 3 min, followed by a final extension at 68 °C for 7 min. Following PCR, 1 μl of DpnI enzyme was added to the reaction and incubated at 37 °C for 1 h to digest the parental supercoiled dsDNA. Mutated plasmids were transformed into XL10-Gold Ultracompetent cells (200315, Agilent Technologies, Inc.) and plated onto LB plates with ampicillin (100 μg/ml) for GST-PRMT9 mutants and GST-SF3B2 mutants or kanamycin (30 μg/ml) (Fisher, catalog no. BP906) for GFP-PRMT9. DNA sequencing on both strands confirmed the mutations in positive colonies (GeneWiz, San Diego).

Generation of a Stable Cell Line Expressing Wild Type and Mutant GFP-PRMT9—Wild type and mutant GFP-PRMT9 on plasmid pEGFP-N1 (7) were transfected into HEK293 Flp-In TREx cells (Invitrogen, catalog no. R780-07). Approximately 1 μg of wild type or mutant plasmid DNA was incubated with 50

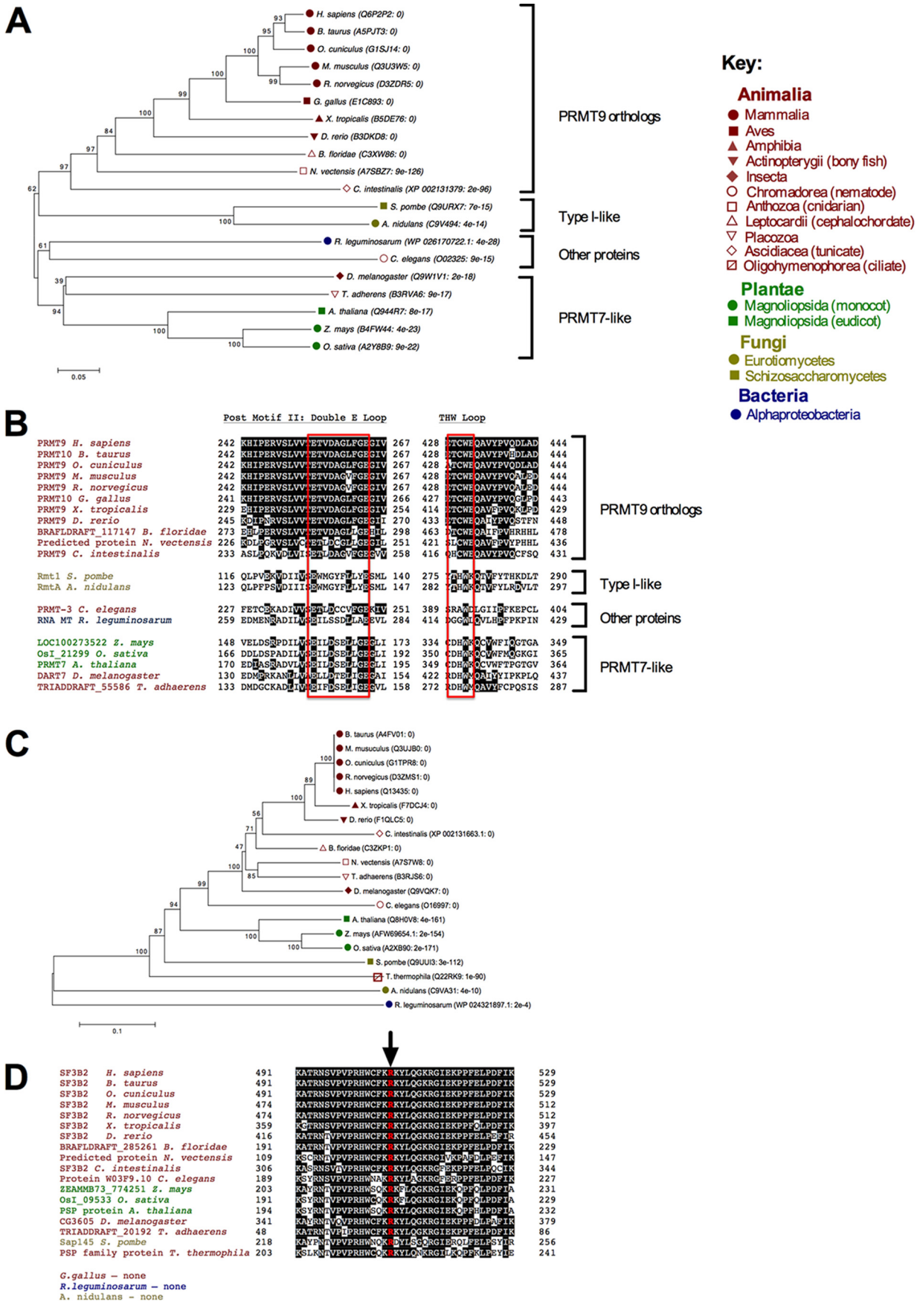
A
H. sapiens (Q6P2P2: 0)
B. taurus (A5PJT3: 0)
O. cuniculus (G1SJ14: 0)
M. musculus (Q3U3W5: 0)
R. norvegicus (D3ZDR5: 0)
G. gallus (E1C893: 0)
X. tropicalis (B5DE76: 0)
D. rerio (B3DKD8: 0)
B. floridae (C3XW86: 0)
N. vectensis (A7SBZ7: 9e-126)
C. intestinalis (XP 002131379: 2e-96)
S. pombe (Q9URX7: 7e-15)
A. nidulans (C9V494: 4e-14)
R. leguminosarum (WP 026170722.1: 4e-28)
C. elegans (O02325: 9e-15)
D. melanogaster (Q9W1V1: 2e-18)
T. adherens (B3RVA6: 9e-17)
A. thaliana (Q944R7: 8e-17)
Z. mays (B4FW44: 4e-23)
O. sativa (A2Y8B9: 9e-22)
0.05
PRMT9 orthologs
Type I-like
Other proteins
PRMT7-like
Key:
Animalia
Mammalia
Aves
Amphibia
Actinopterygii (bony fish)
Insecta
Chromadorea (nematode)
Anthozoa (cnidarian)
Leptocardii (cephalochordate)
Placozoa
Ascidiacea (tunicate)
Oligohymenophorea (ciliate)
Plantae
Magnoliopsida (monocot)
Magnoliopsida (eudicot)
Fungi
Eurotiomycetes
Schizosaccharomycetes
Bacteria
Alphaproteobacteria
B
Post Motif II: Double E Loop
THW Loop
PRMT9 H. sapiens
PRMT10 B. taurus
PRMT9 O. cuniculus
PRMT9 M. musculus
PRMT9 R. norvegicus
PRMT10 G. gallus
PRMT9 X. tropicalis
PRMT9 D. rerio
BRAFLDRAFT_117147 B. floridae
Predicted protein N. vectensis
PRMT9 C. intestinalis
Rmt1 S. pombe
RmtA A. nidulans
PRMT-3 C. elegans
RNA MT R. leguminosarum
LOC100273522 Z. mays
OsI_21299 O. sativa
PRMT7 A. thaliana
DART7 D. melanogaster
TRIADDRAFT_55586 T. adhaerens
PRMT9 orthologs
Type I-like
Other proteins
PRMT7-like
C
B. taurus (A4FV01: 0)
M. musculus (Q3UJB0: 0)
O. cuniculus (G1TPR8: 0)
R. norvegicus (D3ZMS1: 0)
H. sapiens (Q13435: 0)
X. tropicalis (F7DCJ4: 0)
D. rerio (F1QLC5: 0)
C. intestinalis (XP 002131663.1: 0)
B. floridae (C3ZKP1: 0)
N. vectensis (A7S7W8: 0)
T. adhaerens (B3RJS6: 0)
D. melanogaster (Q9VQK7: 0)
C. elegans (O16997: 0)
A. thaliana (Q8H0V8: 4e-161)
Z. mays (AFW69654.1: 2e-154)
O. sativa (A2XB90: 2e-171)
S. pombe (Q9UUI3: 3e-112)
T. thermophila (Q22RK9: 1e-90)
A. nidulans (C9VA31: 4e-10)
R. leguminosarum (WP 024321897.1: 2e-4)
0.1
D
SF3B2 H. sapiens
SF3B2 B. taurus
SF3B2 O. cuniculus
SF3B2 M. musculus
SF3B2 R. norvegicus
SF3B2 X. tropicalis
SF3B2 D. rerio
BRAFLDRAFT_285261 B. floridae
Predicted protein N. vectensis
SF3B2 C. intestinalis
Protein W03F9.10 C. elegans
ZEAMMB73_774251 Z. mays
OsI_09533 O. sativa
PSP protein A. thaliana
CG3605 D. melanogaster
TRIADDRAFT_20192 T. adhaerens
Sap145 S. pombe
PSP family protein T. thermophila
G.gallus – none
R.leguminosarum – none
A. nidulans - none

μl of Opti-MEM (Gibco, Invitrogen, catalog no. 31985062) for 5 min and then added to a solution containing 50 μl of Opti-MEM and 20 μl of FuGENE 6 transfection reagent (Promega, catalog no. E2691). The transfection solution was incubated for 20 min and added to the center of a 6-cm plate containing HEK293 cells in F-12/DMEM (1:1) (HyClone, Thermo Scientific, catalog no. SH30023.02), 10% fetal bovine serum (Tet-tested FBS, Gibco, catalog no. 16000), and 1% penicillin/streptomycin (Invitrogen, catalog no. 15140-122). Plates were incubated at 37 °C, 5% CO_2 for 4 days until the cells were about 80% confluent. At that time, 400 μg/ml geneticin (G418, Invitrogen, catalog no. 11811023) was added, and selection was monitored for 2 weeks. Cells positive for GFP-PRMT9 were confirmed by their ability to form colonies, their fluorescence, and by immunoblotting using an antibody to GFP (anti-rabbit GFP, Abcam).

Immunoprecipitation from HEK293 Cells Expressing GFP-PRMT9—Stable cell lines containing wild type and mutant GFP-PRMT9 DNA were grown to confluence in 1-liter roller bottles with DMEM, 10% Tet-tested FBS, and 1% penicillin/streptomycin. Cells were harvested and washed once with PBS. 220 μg of anti-rabbit GFP antibody (Abcam) was cross-linked to protein A beads (catalog no.156-0006, Bio-Rad) with 0.22 M dimethyl pimelimidate-HCl (Thermo Scientific, catalog no.21667) in 0.2 M sodium borate, pH 9.0. Beads were washed with 0.2 M ethanolamine and 0.2 M NaCl, pH 8.5, to inactivate residual cross-linker. Cells were lysed with LAP300 buffer (50 mM potassium HEPES, pH 7.4, 300 mM KCl, 1 mM EGTA, 1 mM $MgCl_2$, 10% glycerol, 0.3% Nonidet P-40) and protease inhibitor mixture (cOmplete, Roche Applied Science, catalog no.11697498001). The lysate was centrifuged at 28,400 × *g* for 10 min at 4 °C. The supernatant was then spun at 100,000 × *g* for 1 h at 4 °C, and this supernatant was collected and added to 0.4 ml of a 50% slurry of the GFP-protein A beads prepared as described above and equilibrated in LAP200 buffer (same as the LAP300 buffer described above but with 200 mM KCl). After incubation for 1 h at 4 °C, the beads were washed three times with LAP200 and stored in LAP100 buffer (100 mM KCl) at 4 °C.

Immunofluorescence and Localization of GFP-PRMT9 Wild Type and Mutant—Stable cell lines containing wild type and mutant GFP-PRMT9 in HEK293 cells were grown to confluency at 37 °C, 5% CO_2 on a poly-L-lysine-coated coverslip (BD Biosciences, catalog no. 354085) in a 24-well plate. After reaching confluency, cells were fixed using BRB80 buffer (0.4 M PIPES, 5 mM $MgCl_2$, and 5 mM EGTA, pH 6.8) with 4% paraformaldehyde (Electron Microscopy Science, catalog no. 15710). Cells were washed with PBS and permeabilized using 0.2% Triton X-100 for 1 min. Coverslips were then transferred to a moisture chamber and incubated for 30 min at room temperature with immunofluorescence (IF) buffer (PBS containing 5% fish gelatin (Sigma, G7765) and 0.1% Triton X-100). Antibodies were diluted in IF buffer and incubated for 1 h at room temperature. Antibodies used include anti-GFP (rabbit, 1:500) (Abcam) and Hoechst dye 33342 (1:1000) (Invitrogen, catalog no. H1399). Secondary donkey anti-rabbit fluorescein isothiocyanate (FITC) antibody (AffiniPure, Jackson ImmunoResearch, catalog no. 711-095-152) was also diluted (1:500) in IF buffer and incubated at room temperature for 30 min. Coverslips were then washed once with PBS, and 200 μl of anti-fade mounting solution (ProLong gold antifade mounting solution, Invitrogen, catalog no. P36934) was placed on the coverslips and sealed with clear nail polish. Cells were imaged at ×1000 magnification using a Leica TCS SPE I DMI4000 B inverted scanning confocal microscope with a Leica DFC360FX digital camera. Fixed cells on coverslips were kept at 25 °C during imaging. Images were acquired using Leica AF6000 software and analyzed using Fiji ImageJ software (National Institutes of Health).

LC-MS/MS to Identify Substrates and Interaction Partners—Immunoprecipitated GFP-PRMT9 wild type and catalytic mutant samples were sent to the Birmingham Proteomics and Mass Spectrometry Consortium, University of Alabama at Birmingham, for protein identification. Data were received as summary of protein peptide hits, among which were sorted for the top protein peptide hits identified and used in this study.

Amino Acid Analysis of Substrates Using High Resolution Cation Exchange Chromatography—In vitro methylation reactions included the indicated amount of enzyme and substrate proteins and 0.7 μM *S*-adenosyl-L-[*methyl*-^{3}H]methionine ([*methyl*-^{3}H]AdoMet; PerkinElmer Life Sciences, 75–85 Ci/mmol, 0.55 mCi/ml in 10 mM H_2SO_4/EtOH (9:1, v/v)) in a total volume of 60 μl. The reactions were performed at 37 °C in 50 mM potassium HEPES, 10 mM NaCl, and 1 mM DTT, pH 8.0. Reactions were stopped by adding trichloroacetic acid to 12.5% with 20 μg of the carrier protein bovine serum albumin. Acid hydrolysis and high resolution cation exchange chromatography were then performed as described previously (7). For ninhydrin assay, 50 μl of each fraction from the cation exchange column was used to determine the elution of nonradiolabeled standards, and the rest of the fraction (950 μl) was used for liquid scintillation counting. The efficiency of counting was determined to be about 51%. Under these conditions, about 90 cpm correspond to 1 fmol of radiolabeled methyl groups.

Detection of Methylated Substrates after SDS-PAGE—Methylation reactions were set up as described above for the amino acid analysis, but the reactions were quenched by the addition of SDS loading buffer. Reactions were then boiled for 5 min at 100 °C and separated on 12.6% Tris-glycine gels or 4–12% Bis-tris gel (NuPAGE Novex, Invitrogen, NP0335BOX), stained

FIGURE 1. **Evolutionary conservation of PRMT9 and SF3B2.** *A* and *C,* representative phylogenetic trees based on human PRMT9 (Q6P2P2) (*A*) and human SF3B2 (Q13435) (*C*) are shown for the selected organisms. UniProt IDs of top ranked orthologs with their respective *E* value are shown. The percentage of replicate trees in which the specific associated taxa clustered together in 500 replicates of the boot strap test is shown next to the branches. Evolutionary distances are displayed in units of the number of amino acid differences per site. All proteins were mutual best hits, and all organisms have complete genomes sequenced. Based on groupings in the phylogenetic tree, proteins were identified as "*PRMT9 orthologs*," "*type I-like*," "*other proteins*," and "*PRMT7-like*." *B,* sequence alignment of post-motif II; double E loop and THW loop residues, the two major distinguishing motifs found in PRMTs. *Shaded letters* indicate sequence identity. Double E loop residues and THW loop residues are *boxed* in *red*. *D,* sequence alignment of amino acids surrounding the Arg-508 site that is methylated by PRMT9. *Shaded letters* indicates sequence identity, using the same species, order and UniProt IDs as indicated in *C*. The Arg-508 methylation site indicated in *red* and an *arrow*.

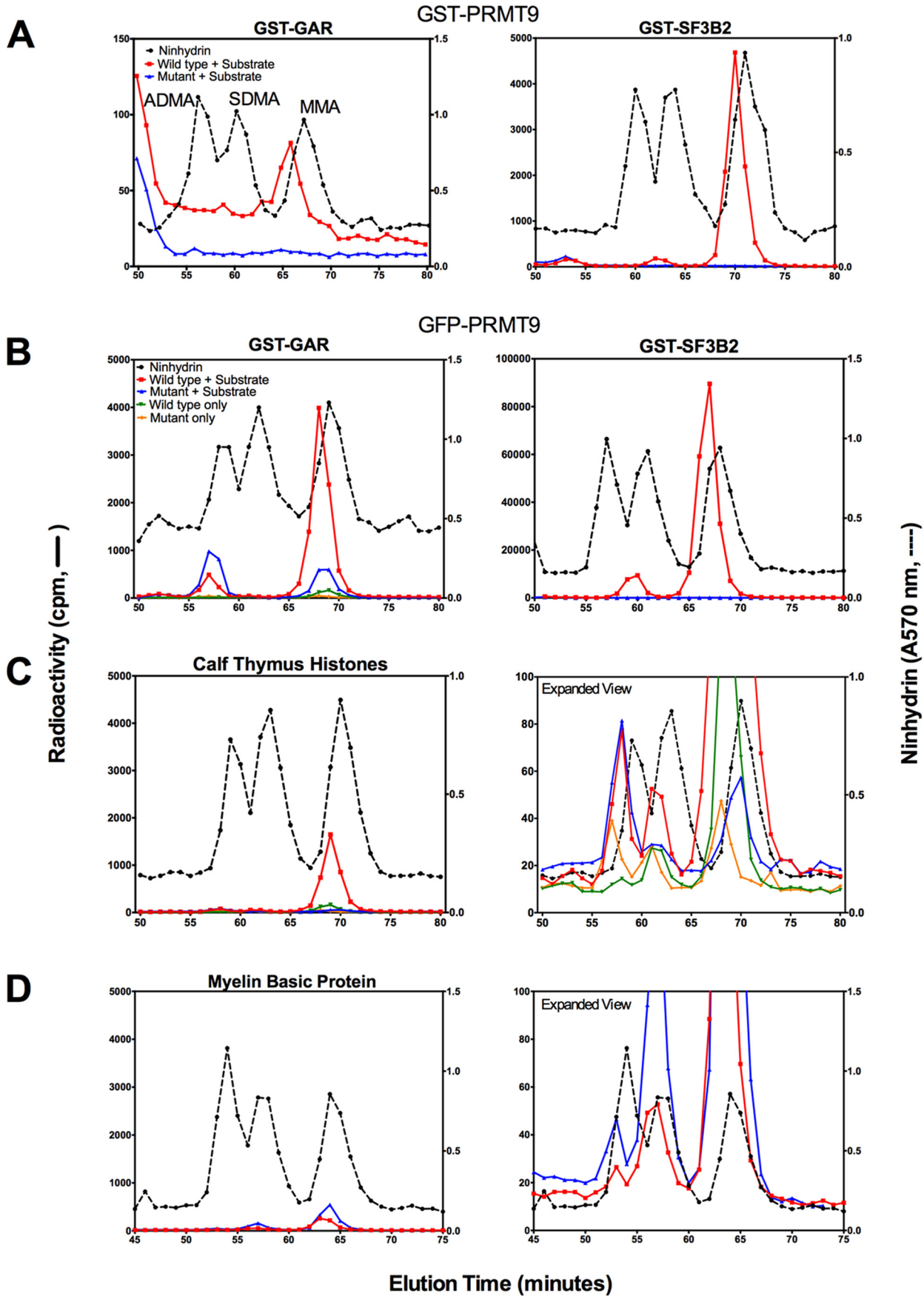
A
GST-PRMT9
GST-GAR
GST-SF3B2
Ninhydrin
Wild type + Substrate
Mutant + Substrate
ADMA
SDMA
MMA
B
GFP-PRMT9
GST-GAR
GST-SF3B2
Ninhydrin
Wild type + Substrate
Mutant + Substrate
Wild type only
Mutant only
C
Calf Thymus Histones
Expanded View
D
Myelin Basic Protein
Expanded View
Radioactivity (cpm, —)
Ninhydrin (A570 nm, ----)
Elution Time (minutes)

with Coomassie Blue for 1 h, and destained overnight. After destaining, the gel was treated with autoradiography enhancing buffer (EN^{3}HANCE, PerkinElmer Life Sciences, catalog no. 6NE9701) and vacuum dried. The dried gel was then exposed to autoradiography film (Denville Scientific, catalog no. E3012) at −80 °C for the indicated amount of time. For radioactive gel slice assay, gels were prepared, enhanced, and dried as described above, but the dried gel band was cut and submerged in 30% H_2O_2 for 24 h at 37 °C in a scintillation vial to solubilize. After incubation, 10 ml of Safety-Solve scintillation mixture (Research Products International, catalog no. 111177) was added to the vial, which was then counted for three 5-min cycles on a Beckman LS6500 liquid scintillation instrument. As described above, the specific activity of the label was about 90 cpm/fmol.

Generation of a PRMT5 Inducible Knock-out Cell Line—PRMT5 floxed mice were crossed with ER-Cre mice to generate *Prmt5$^{F/F}$*ER embryos and subsequently mouse embryonic fibroblasts (MEFs), as described previously (28). The MEFs, kindly provided by Drs. Marco Bezzi and Ernesto Guccione, were immortalized by maintaining cells on a 3T3 culture protocol in which 10^6 cells were passed onto gelatinized 10-cm dishes every 3 days.

PRMT5 Knock-out MEFs and Immunoblotting—To knock out PRMT5, Prmt5$^{F/F}$ER MEFs were treated with 2 μM 4-hydroxytamoxifen (OHT) for 14 or 30 days. Whole cell lysates of OHT-treated and untreated MEFs were separated by SDS-PAGE and transferred onto PVDF membranes. Blots were probed with a panel of antibodies, including anti-PRMT5 (1:1000) (Millipore), anti-SDMA (BL8243, 1:500) (Cell Signaling Technology, CST), anti-SDMA (BL8244, 1:200) (CST), anti-ADMA (D10F7, 1:2000)(CST), anti-MMA (1:2000, CST, catalog no. 8711), and anti-actin (1:10000) (Sigma, catalog no. A1978).

Amino Acid Analysis of Protein Hydrolysates and Quantification of SDMA—Approximately 40 mg of wet weight MEFs and 100 μl of 6 N HCl were added to a 6 × 50-mm glass tube and acid-hydrolyzed *in vacuo* as described above. After hydrolysis, the lysates were vacuum dried and resuspended in 100 μl of water and centrifuged at maximum speed (20,000 × *g*) for 10 min to remove debris. 75 μl was added to 250 μl of citrate loading buffer (0.2 M Na^+, pH 2.2), and amino acids were separated using the high resolution cation exchange chromatography method described above. Individual fractions collected with the known elution positions of ADMA, SDMA, MMA, and arginine were further derivatized using OPA for fluorescence detection and quantification using separation on a reverse phase HPLC (HP 1090 II liquid chromatograph coupled to a Gilson model 121 fluorometer with excitation filter of 305–395 nm and emission filter of 430–470 nm, with a setting of 0.001 relative fluorescence units), as described previously (29). An Agilent ZORBAX Eclipse AAA (analytical, 5 μm, 4.6-mm inner diameter, 150 mm in length) reverse phase column was used with 25-μl sample injection volumes at 32 °C and a flow rate of 1.7 ml/min. Solvent A consisted of 50 mM sodium acetate, pH 7.0, and solvent B of 100% methanol. The HPLC gradient used to separate the methylated OPA derivatives included a shallow gradient from 23 to 31.5% B for 20 min, a 5-min hold at 95% B, and a 14-min hold at 23% B. Because fractions containing arginine OPA derivatives commonly overloaded the detector, dilutions were made in the eluting buffer of the cation exchange column (sodium citrate, pH 5.25). The elution positions of methylated arginine derivatives were confirmed by comparison with standards. To quantify the data, the area under the curve for each amino acid peak of interest was determined using Excel by integration and area of summation by trapezoids. The total amount of each modification was calculated by summing the area of each cation exchange fraction that had the methylated amino acid present. Each replicate was normalized to cellular levels of arginine.

Results

Human PRMT9 and SF3B2 (SAP145) Are Evolutionarily Conserved among Vertebrates and Invertebrates—A BLAST search was used to identify homologs of human PRMT9 and SF3B2 in vertebrates, invertebrates, plants, and fungi. The sequences were aligned using MUSCLE, and a phylogenetic tree was assembled to show the conservation across various species (Fig. 1, *A* and *C*). Alignment of the post-motif II substrate-binding double E loop shows a clear conservation of the acidic residue Asp-258 and Gly-260 across all PRMT9 orthologs (Fig. 1*B*). Divergent sequences included PRMT7-like sequences in plants and invertebrates (Fig. 1*B*). Alignment of the THW loop also shows conservation of a cysteine residue in

FIGURE 2. **PRMT9 does not or very weakly methylates common PRMT substrates.** *A,* amino acid analysis of ^{3}H methylation reaction of bacterially expressed GST-PRMT9 wild type and catalytic mutant with GST-GAR (*left*) and GST-SF3B2 401–550-residue fragment (*right*) after 20 h of reaction at 37 °C, with 0.7 μM [*methyl*-^{3}H]AdoMet, and reaction buffer of 50 mM HEPES, 10 mM NaCl, 1 mM DTT, pH 8.0, in a final reaction volume of 60 μl. Approximately 5 μg of each substrate was reacted with 2 μg of wild type and catalytic mutant GST-PRMT9 enzyme. After TCA precipitation and acid hydrolysis, 1 μmol of ADMA, SDMA, and MMA standards were added, and amino acid analysis was carried out as described under "Experimental Procedures." The *dotted black line* indicates the ninhydrin absorbance at 570 nm for the elution of the nonradiolabeled standards. The *red line* indicates the elution of radioactive methylated amino acids from the reaction of the wild type enzyme with substrate, and the *blue line* indicates the elution of radioactive methylated amino acids from the methylation reaction of the catalytic mutant enzyme with the substrate. Radioactivity is given as the average of three counting cycles on a liquid scintillation counter. Because of the tritium isotope effect, radioactive methylated amino acids elute about 1 min prior to the nonisotopically labeled standards (45). *B,* amino acid analysis of methylation reactions of a more active mammalian-expressed GFP-PRMT9, with GST-GAR (*left*) and GST-SF3B2 401–550-residue fragment (*right*) after a 20-h reaction, using the same reaction conditions described in *A*. Approximately 5 μg of GST-GAR and GST-SF3B2 401–550-residue fragment were used in methylation reactions with 1 μg of GFP-PRMT9 wild type or catalytic mutant. The *red line* indicates the elution of radioactive methylated amino acids from the reaction of the wild type GFP-PRMT9 enzyme with the substrate. The *blue line* indicates the elution of the radioactive methylated amino acids from the reaction of the catalytic mutant GFP-PRMT9 enzyme with the substrate. The *green* and *orange lines* indicate the wild type and mutant enzyme only controls, respectively, showing any radioactivity due to background contamination in the GFP-PRMT9 enzymatic preparations. *C,* amino acid analysis of methylation reactions of 1 μg of GFP-PRMT9 wild type or catalytic mutant with 5 μg of calf thymus histones (*left*) after 20 h, using the same reaction conditions described above. *Right panel* is an expanded view of the radioactivity scale to show residual activity with the control reactions. *D,* amino acid analysis of methylation reactions of 1 μg of GFP-PRMT9 wild type or catalytic mutant preparations with 10 μg of bovine-purified MBP after 1 h (*left panel*), using the same reaction conditions described above. *Right panel* shows an expanded view of the radioactivity scale to show residual activity of the control reaction with the catalytic mutant.

A

Top Hits: (>5 peptide matches)	Species	UniProt ID	UniProt #	Size	Peptide Matches
60 kDa heat shock protein, mitochondrial	Homo sapiens	CH60_HUMAN	P10809	61 kDa	8
ATP synthase subunit alpha, mitochondrial	Hominidae	ATPA_HUMAN	P25705	60 kDa	11
DNA-dependent protein kinase catalytic sut	Homo sapiens	PRKDC_HUMAN	P78527	469 kDa	13
GFP-PRMT9			**GB0003**	**94 kDa**	**18**
Heat shock 70 kDa protein 1A/1B	Catarrhini	HSP71_HUMAN	P08107	70 kDa	8
Heat shock cognate 71 kDa protein	Eutheria	HSP7C_HUMAN	P11142	71 kDa	9
Heat shock protein HSP 90-beta	Homo sapiens	HS90B_HUMAN	P08238	83 kDa	5
Insulin receptor substrate 4	Homo sapiens	IRS4_HUMAN	O14654	134 kDa	5
Serum albumin	Bos taurus	ALBU_BOVIN	P02769	69 kDa	5
Sodium/potassium-transporting ATPase sut	Homo sapiens	AT1A1_HUMAN	P05023	113 kDa	8
Splicing factor 3B subunit 2	Hominidae	SF3B2_HUMAN	Q13435	100 kDa	21
Splicing factor 3B subunit 4	Catarrhini	SF3B4_HUMAN	Q15427	44 kDa	2
Translational activator GCN1	Homo sapiens	GCN1L_HUMAN	Q92616	293 kDa	5
Tubulin alpha-1B chain	Tetrapoda	TBA1B_HUMAN	P68363 (+1)	50 kDa	7
Tubulin beta chain	Amniota	TBB5_HUMAN	P07437	50 kDa	8

B

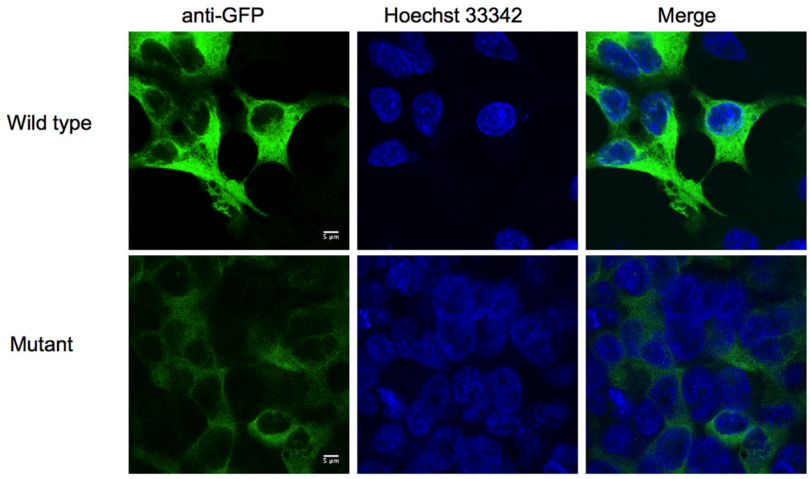

C

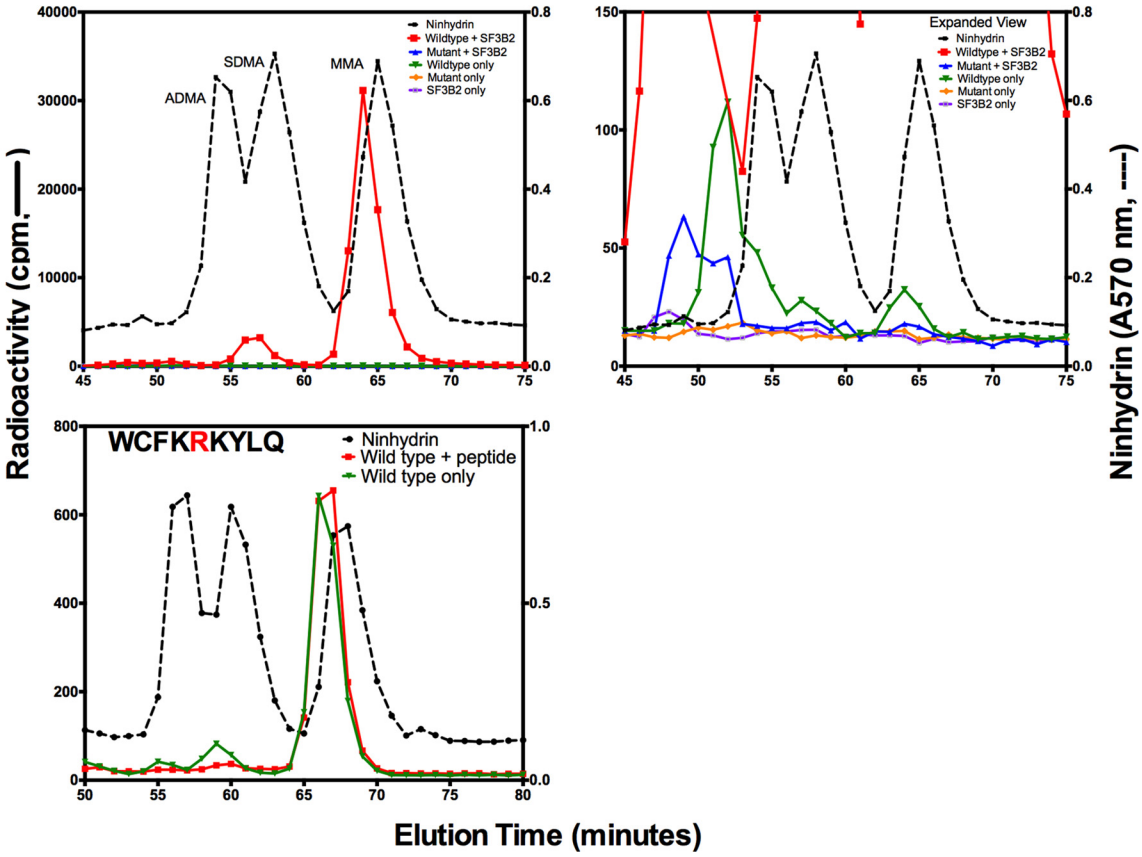

D

Elution Time (minutes)

place of a histidine residue that is found in other types of PRMTs (Fig. 1*B*). Interestingly, the only other mammalian PRMT with a non-histidine residue at this position is PRMT5 (serine); the presence of smaller residues at this site has been suggested to correlate with the ability of PRMT5 and PRMT9 to form SDMA (4).

In our previous work, we identified Arg-508 on SF3B2 to be the target methylation site for PRMT9 (7). Analysis of the sequence surrounding Arg-508 of SF3B2 shows a strict conservation of this residue and the surrounding residues in vertebrates, invertebrates, plants, and fungi (Fig. 1*D*). The Lys-507 and Lys-509 residues are conserved in almost all species (Fig. 1*D*), with the exception of *Schizosaccharomyces pombe*, where the second lysine is replaced with an aspartate. Aromatic residues of Phe-506 and Tyr-510 are also well conserved, with differences found in the plants. Interestingly, the chicken *Gallus gallus* contains a PRMT9 ortholog, but an ortholog of SF3B2 does not appear to exist. In addition, *Nematostella vectensis* (a sea anemone) contains a PRMT9 ortholog, but this gene seems to have been lost in other species of the same phyla. In addition, organisms such as the fungi *Aspergillus nidulans* and the bacterium *Rhizobium leguminarosum* contain an SF3B2 ortholog but do not appear to have an ortholog of PRMT9, suggesting the enzyme plays a role unique to higher eukaryotes. The nematode *C. elegans* PRMT-3 protein (UniProt O02325 in Fig. 1*A*) is noteworthy because it is most closely related to PRMT9 (30), yet published studies show that it generates only MMA (31).

PRMT9 Is Poorly Active on Bona Fide PRMT Substrates—Most PRMTs are able to efficiently methylate a variety of substrate proteins; PRMT1 and PRMT5 have very broad substrate specificity, whereas PRMT4, PRMT6, and PRMT8 have a more limited specificity but still methylate a variety of substrates (2). We thus tested whether recombinant PRMT9 can methylate the common substrates of these other PRMTs, including a recombinant GST fusion of the N-terminal glycine and argi nine-rich region of fibrillarin (GST-GAR) that is recognized by PRMT1, PRMT3, and PRMT5–7 (2, 3, 8, 27, 32). In contrast to other PRMTs, we found that PRMT9 poorly methylates GST-GAR, as shown by amino acid analysis, with only a small radioactive MMA peak formed (Fig. 2*A*, *left panel*). Not surprisingly, PRMT9 is highly active on its biological substrate as the GST-SF3B2 401–550-residue fragment (Fig. 2*A*, *right panel*), producing both MMA (100-fold higher than GST-GAR) as well as SDMA products. A more active preparation of mammalian-expressed PRMT9 (GFP-PRMT9) proved to have enhanced methyltransferase activity on GST-GAR (Fig. 2*B*, *left panel*) and GST-SF3B2 (Fig. 2*B*, *right panel*), where both MMA (20-fold higher with GST-SF3B2 than that seen with GST-GAR) and SDMA were formed. Calf thymus histones were weakly methylated by the GFP-PRMT9 enzyme (MMA and some SDMA, Fig. 2*C*) but not to the level seen with SF3B2. MBP could not be methylated by PRMT9, as no activity was seen above that observed in the catalytic mutant (Fig. 2*D*). Here, the catalytically inactive GFP-PRMT9 was used as a control to rule out the possibility of another PRMT contaminant coimmunoprecipitating with the mammalian-expressed enzyme. We conclude that PRMT9 has little to no activity on the broadly methylated known substrates of the other mammalian PRMTs, and it appears to be relatively specific for the splicing factor SF3B2.

Mammalian-expressed PRMT9 Copurifies with Its Methylation Substrate SF3B2 and Is Localized to the Cell Cytoplasm—Mass spectrometry analysis of tryptic peptides was done on the immunoprecipitated wild type and catalytically inactive GFP-PRMT9 expressed in neuronally derived HEK293 cells (33) for protein identification of other possible binding partners and/or substrates. We previously showed that tandem affinity purification-tagged PRMT9 expressed in cervically derived HeLa cells was associated with SF3B2 and SF3B4 (7), and we sought to confirm this interaction with a different cell type. In HEK293 cells, wild type PRMT9 was associated with several proteins commonly brought down during the purification process but most interestingly brought down SF3B2 (SAP145) and SF3B4 (SAP49) as the top hits (Fig. 3*A*). Mass spectrometry analysis on the catalytic mutant GFP-PRMT9 did not identify any SF3B2 or SF3B4 peptides (data not shown), possibly suggesting that the binding of AdoMet is a prerequisite for complex formation or substrate binding. Immunofluorescence of wild type and mutant PRMT9 confirms the protein is primarily found in the cytoplasm, with some possible nuclear localization (Fig. 3*B*, *top panels*). Tissue-based mapping of the human proteome (34) confirms this localization, perhaps suggesting that variation of localization and expression is based on the cell type. The GFP-PRMT9 mutant protein was expressed in much lower

FIGURE 3. **Interaction partner identification, localization, and activity characterization of mammalian expressed PRMT9.** Mammalian expressed wild type and catalytic mutant GFP-PRMT9 constructs were immunoprecipitated from HEK293 cells as described under "Experimental Procedures." *A,* LC-MS/MS analysis was done on immunoprecipitated wild type and catalytic mutant GFP-PRMT9 samples to identify possible substrates and interaction partners. Identified peptide hits with greater than five peptide matches are listed (with the exception of SF3B4 with two peptide hits but was important for our analysis) for the wild type enzyme preparation, along with their UniProt ID and number, molecular weight, and the exact number of peptide hits. Catalytic mutant GFP-PRMT9 had similar peptide matches (data not shown), with the exception of the two splicing factors SF3B2 and SF3B4 identified in the wild type preparation were not identified with the mutant sample. *B,* immunofluorescence experiments to determine the intracellular localization of the wild type and catalytic mutant GFP-PRMT9 samples. Immunofluorescence was performed in HEK293 cells using anti-GFP antibody at 1:500 dilution. The *scale bar* indicates 5 μm. *C,* amino acid analysis (described under "Experimental Procedures" (7)) of methylation reactions with GFP-PRMT9 wild type or catalytic mutant enzymes and GST-SF3B2 401–550-residue fragment after 1 h at 37 °C. Approximately 1 μg of enzyme was reacted with 5 μg of substrate, in a final reaction volume of 60 μl consisting of 0.7 μM [*methyl*-^{3}H]AdoMet and reaction buffer of 50 mM HEPES, 10 mM NaCl, 1 mM DTT, pH 8.0. *Right panel* displays the expanded view of the radioactivity scale to show residual activity of the control reactions with the catalytic mutant and enzyme and substrate only controls. The *black dotted line* indicates the ninhydrin absorbance at 570 nm for the elution of the nonradiolabeled standards. The *solid line* indicates the elution of the radioactive methylated amino acids after the reaction of the enzyme with the substrate (*red*, wild type GFP-PRMT9, and *blue*, catalytic mutant GFP-PRMT9). The *green* and *orange lines* indicate the wild type and catalytic mutant GFP-PRMT9 enzyme only controls, respectively, and the *purple line* indicates the substrate only control. *D,* amino acid analysis of a highly active HA-tagged PRMT9 with a synthetic peptide consisting of the Arg-508 methylation site (highlighted in *red*), WCFKRKYLQ, indicated in the figure. The methylation reaction consisted of ~1 μg of HA-tagged PRMT9 and 12.5 μM peptide, 0.7 μM [*methyl*-^{3}H]AdoMet, and methylation reaction buffer of 50 mM HEPES, 10 mM NaCl, 1 mM DTT, pH 8.0, at 37 °C for 18 h. *Green line* indicates the enzyme only control reaction for background contamination.

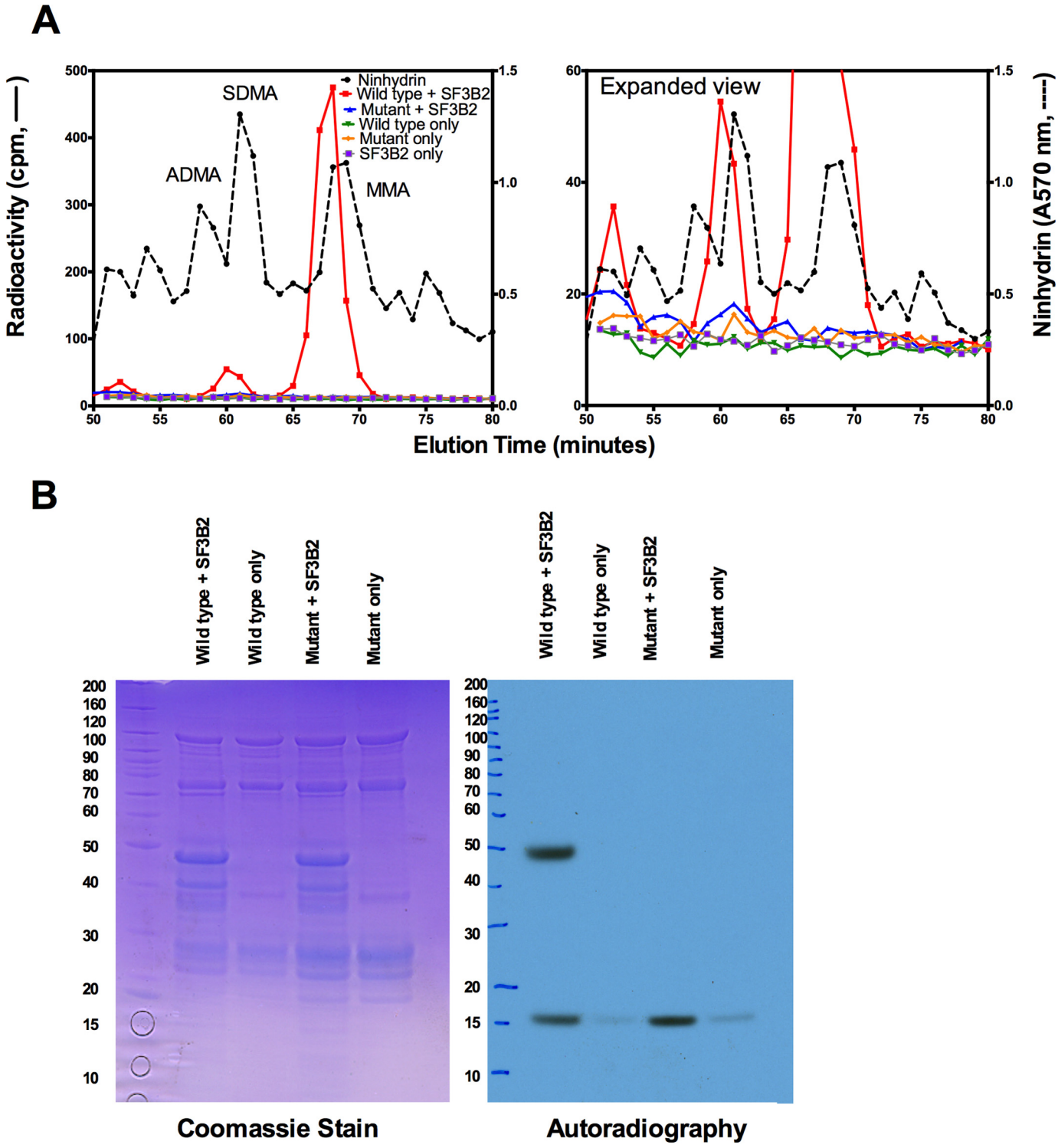

FIGURE 4. **Bacterially expressed GST-PRMT9 is very active on SF3B2 substrate.** *A,* amino acid analysis (described under "Experimental Procedures" (7)) using bacterially expressed GST-PRMT9 with GST-SF3B2 401–550-residue wild type fragment. Methylation reaction consisted of 2 μg of enzyme (wild type or catalytic mutant), 5 μg of GST-SF3B2 401–550-residue fragment, 0.7 μM [*methyl*-^{3}H]AdoMet, and methylation reaction buffer of 50 mM HEPES, 10 mM NaCl, 1 mM DTT, pH 8.0, at 37 °C for 1 h. The *dashed black line* indicates the ninhydrin absorbance at 570 nm for the elution of the nonradiolabeled standards. *Solid lines* indicate the elution of the radioactive methylated amino acids after the reaction of the enzyme with the substrate (*red*, wild type GST-PRMT9, and *blue*, catalytic mutant GST-PRMT9). *Green* and *orange lines* indicate the wild type and catalytic mutant enzyme only controls, respectively. The *purple line* indicates substrate only control. *B,* autoradiography of ^{3}H-methylated GST-SF3B2 401–550-residue fragment with wild type or catalytic mutant GST-PRMT9. Reactions were prepared as described in *A* for 1 h, and autoradiography was prepared as described above under "Experimental Procedures." The dried gel was then exposed to autoradiography film (Denville Scientific, E3012) for 7 days at −80 °C. BenchMark Protein Ladder (Invitrogen, catalog no. 10747-012) was used, with ~0.5 μg of each standard is shown. The identity of a nonspecific radiolabeled band shown at 16 kDa is unknown, but its formation is not dependent upon an active PRMT9 enzyme.

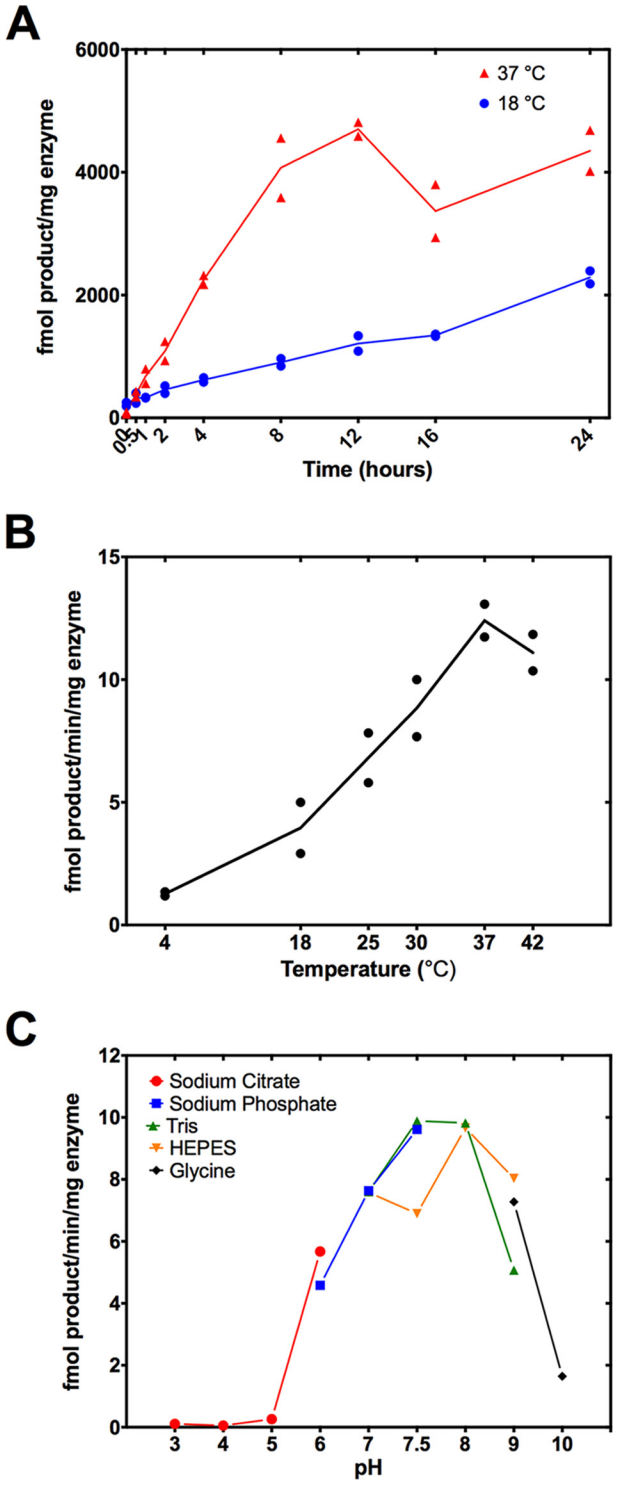

FIGURE 5. **Optimization of reaction conditions for PRMT9.** *A–C,* optimization of reaction conditions with GST-tagged PRMT9 for time (*A*), temperature (*B*), and buffer and pH (*C*). For all optimization conditions, reactions were quenched after the appropriate time by the addition of SDS loading buffer and run on a 12.6% Tris-glycine gel as described under "Experimental Procedures" for radioactive gel slice assay. *A,* time course reaction of GST-PRMT9 wild type enzyme with its substrate GST-SF3B2 401–550-residue wild type fragment. The reactions contained ~4 μg of GST-PRMT9, 6 μg of GST-SF3B2, 0.7 μM [*methyl*-^{3}H]AdoMet in a 60-μl reaction buffer of 50 mM potassium HEPES, pH 8.0, 10 mM NaCl, and 1 mM DTT. The reactions were run in duplicate at the indicated temperature (*red line,* 37 °C; *blue line*, 18 °C) for the indicated time (0, 0.5, 1, 2, 4, 8, 12, 16, and 24 h), run on SDS-PAGE, and counted as described under "Experimental Procedures." The specific activity determined for the [*methyl*-^{3}H]AdoMet (about 90 cpm/fmol) was used to calculate the amount of product formed. *B,* temperature dependence of GST-PRMT9 wild type with GST-SF3B2 401–550-residue wild type fragment. The reactions contained 4 μg of GST-PRMT9, 6 μg of GST-SF3B2, 0.7 μM [*methyl*-^{3}H]AdoMet in a 60-μl reaction buffer of 50 mM potassium HEPES, pH 8.0, 10 mM NaCl, and 1 mM DTT. Duplicate reactions were incubated at the indicated temperature for 18.5 h, run on SDS-PAGE, and counted as described above. The activity was calculated as in *A*. *C,* buffer type and pH influences activity of the enzyme with its substrate. Reactions contained 4 μg of GST-PRMT9 wild type, 6 μg of GST-SF3B2 401–550-residue wild type fragment, 0.7 μM [*methyl*-^{3}H]AdoMet, and the addition of 50 mM buffer (sodium citrate (pH 3.0, 4.0, 5.0, and 6.0, *red line*), sodium phosphate (pH 6.0, 7.0, and 7.5, *blue line*), Tris (pH 7.0, 7.5, 8.0, and 9.0, *green line*), HEPES (pH 7.0, 7.5, 8.0, and 9.0, *orange line*), and glycine (pH 9.0 and 10.0, *black line*)) at a final reaction volume of 60 μl. Reactions were run for 8.5 h at 37 °C. The reactions were quenched and run on a gel as described above and under "Experimental Procedures." Solubilized gel slices were counted and activity calculated as in *A*.

amounts (Fig. 3*B*, *bottom panels*), suggesting it may not be as stable as the wild type fusion protein. These localization studies suggest that PRMT9 methylates its substrate primarily in the cytoplasm, before SF3B2 is shuttled to the nucleus to participate in splicing. Amino acid analysis of GFP-PRMT9 with the bacterially expressed GST-SF3B2 fragment containing the methylation site (7) shows great methylation activity after only 1 h (Fig. 3*C*), with the controls of mutant enzyme, enzymes alone, or substrate alone showing negligible activity.

Our previous work has shown the site of PRMT9 methylation on SF3B2 is at Arg-508 (7). To study the effect of residues adjacent to Arg-508 on the methyltransferase activity of PRMT9, a synthetic peptide containing the SF3B2 sequence of residues 504–512 WCFKRKYLQ was generated (GenScript) and tested as a methyl-acceptor for PRMT9. Surprisingly, both GFP-PRMT9 (data not shown) and an even more active insect-expressed HA-tagged PRMT9 showed no activity above the enzyme only control (Fig. 3*D*). Other peptides derived from histone H2B and H4 residues and their mutants (H2B(23–37), H4(1–21), and H4(14–22) (6, 8)) containing a similar KRK sequence found in SF3B2 were also tested, and again no methylation activity was detected (data not shown). These results suggest that a specific conformation of the protein around the methylated arginine residue is required for PRMT9 methylation.

Bacterially Expressed GST-PRMT9 SDMA Forming Activity on Splicing Factor SF3B2—Because mammalian-expressed enzymes may be contaminated with endogenous PRMT family members, and because it is generally accepted that no PRMT activity has been observed in *E. coli* and other eubacteria (35–37), we bacterially expressed the GST-PRMT9 enzyme to further test for methylation activity. Using the GST-SF3B2 401–550-residue fragment fusion protein as a substrate in *in vitro* reaction mixtures with [*methyl*-^{3}H]AdoMet, we showed the formation of MMA and SDMA products by amino acid analysis (Fig. 4*A*) and the strong methylation of the polypeptide with the wild type enzyme but not with the catalytic mutant (Fig. 4, *A* and *B*). These results further validate SF3B2 as the biological substrate, because such activity with other substrates is not seen with the GST recombinant enzyme (Fig. 2*A*, *left panel,* and data not shown).

To study the effects of active site mutations on the GST-PRMT9 enzyme, we optimized reaction conditions to deter-

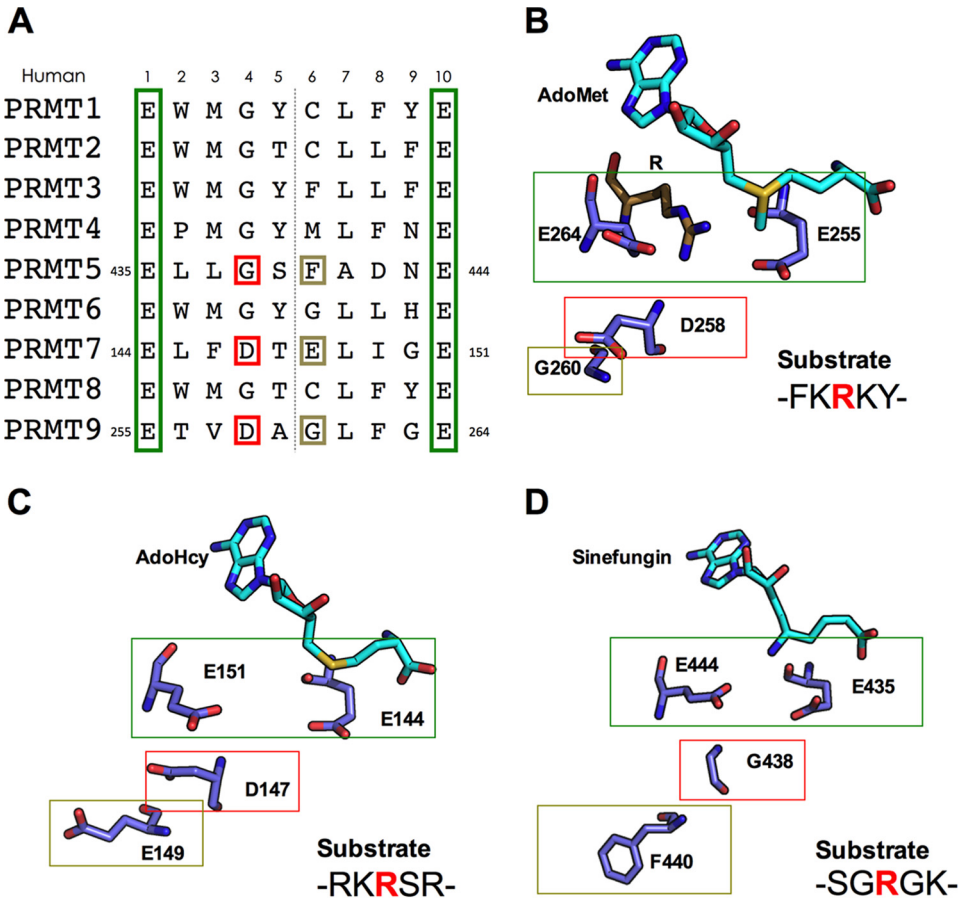

FIGURE 6. **Comparison of the double E loop residues of PRMT9 with known PRMT structures.** *A,* sequence alignment of the double E loop post motif II residues of the nine human PRMTs. The Glu residues making up the double E loop are *boxed* in *green*. Important residues unique to PRMT5, PRMT7, and PRMT9 are *boxed* in *red* and *yellow*. Sequences correspond to PRMT1 (UniProt ID, Q99873), PRMT2 (P55345), PRMT3 (O60678), PRMT4/CARM1 (Q86X55), PRMT5 (O14744), PRMT6 (Q96LA8), PRMT7 (Q9NVM4), PRMT8 (Q9NR22), and PRMT9 (Q6P2P2). *B,* predicted structure of *Homo sapiens* PRMT9 using modeling to other PRMTs with known structures generated by Phyre2.0 software, with AdoMet included as a ligand. A close look at important double E loop substrate-binding motif resides in relation to the AdoMet and substrate Arg. Acidic residues Glu-255 and Glu-264, which make up the ends of the double E loop, are boxed in *green*. Asp-258, in the middle of the double E loop, is boxed in *red*, and Gly-260, a position where other PRMTs have a distinguishing residue and PRMT7 contains a Glu, is *boxed* in *yellow*. The PRMT9 structure was modeled using Phyre2.0 (38) with input sequence from UniProt ID: Q6P2P2 and analyzed using PyMOL software. SF3B2 substrate sequence is listed, with substrate arginine highlighted in *red*. *C,* important residues of the double E loop in the crystal structure of *M. musculus* PRMT7 (Protein Data Bank code 4C4A (16)) with *S*-adenosylhomocysteine as a ligand. Mouse PRMT7 double E loop residues are identical to those of human PRMT7. Glu-144 and Glu-151 residues making up the ends of the double E loop are *boxed* in *green*. Acidic residues Asp-147 and Glu-149 are *boxed* in *red* and *yellow*, respectively. Structure was analyzed using PyMOL software. General substrate sequence is listed, with substrate arginine highlighted in *red*. *D,* a look at important residues of the double E loop in the crystal structure of *H. sapiens* PRMT5 (Protein Data Bank code 4GQB (39)) with sinefungin as a ligand. Gly-438 and Phe-440 in identical positions to those highlighted in *B* and *C* are *boxed* in *red* and *yellow*, respectively. Structure was analyzed using PyMOL software. General substrate sequence is listed, with substrate arginine highlighted in *red*.

mine the best conditions for methylation and also determine the amount of time needed to attain linear product formation. At 37 °C, enzyme activity was linear for 8 h, although at 18 °C it was linear for 12 h. In contrast to the PRMT7 enzyme (8), the activity was found to be ~4-fold higher at 37 °C than at 18 °C. Analysis of enzyme activity over the range of 4–42 °C demonstrated maximal activity at 37 °C (Fig. 5*B*). Using a variety of buffers, we found optimal activity at pH values between 7.5 and 8.0, although significant activity was detected from pH 6.0 to 9.0 (Fig. 5*C*).

Substrate-binding Double E Loop Residues Play an Important Role in Coordinating the Substrate Arginine—PRMTs contain a signature "double E loop" post-motif II, in which two glutamate residues that bind the methylatable arginine residue of the substrate protein are separated by eight residues (EX_8E (2)). Sequence alignment of these residues in the nine human PRMTs shows several conserved residues (Fig. 6*A*). Type I PRMTs (PRMT1–4, PRMT6, and PRMT8) all contain signature WMG or PMG sequences in positions 2–4, where the type II (PRMT5 and PRMT9) and type III (PRMT7) enzymes contain distinct sequences. PRMT7 and PRMT9 each contain an acidic Asp residue at position 4; PRMT7 has an additional acidic residue at position 6, although PRMT9 has a Gly residue there. The acidic residues at positions 4 and 6 have been shown to have an important role in substrate recognition for human PRMT7 (8). The predicted structure of the PRMT9 double E loop using Phyre2.0 modeling (38) shows the relative positions of the glutamate residues (residues 255 and 264) responsible for binding the substrate arginine. In this model, the carboxylate group of the position 4 Asp-258 points away from the substrate arginine, possibly to coordinate the binding of one or both of the two lysine residues adjacent to the methylated arginine in the FKRKY sequence of SF3B2 (Fig. 6*B*). The crystal structure of mouse PRMT7 (Fig. 6*C*) (16) shows a similar positioning of

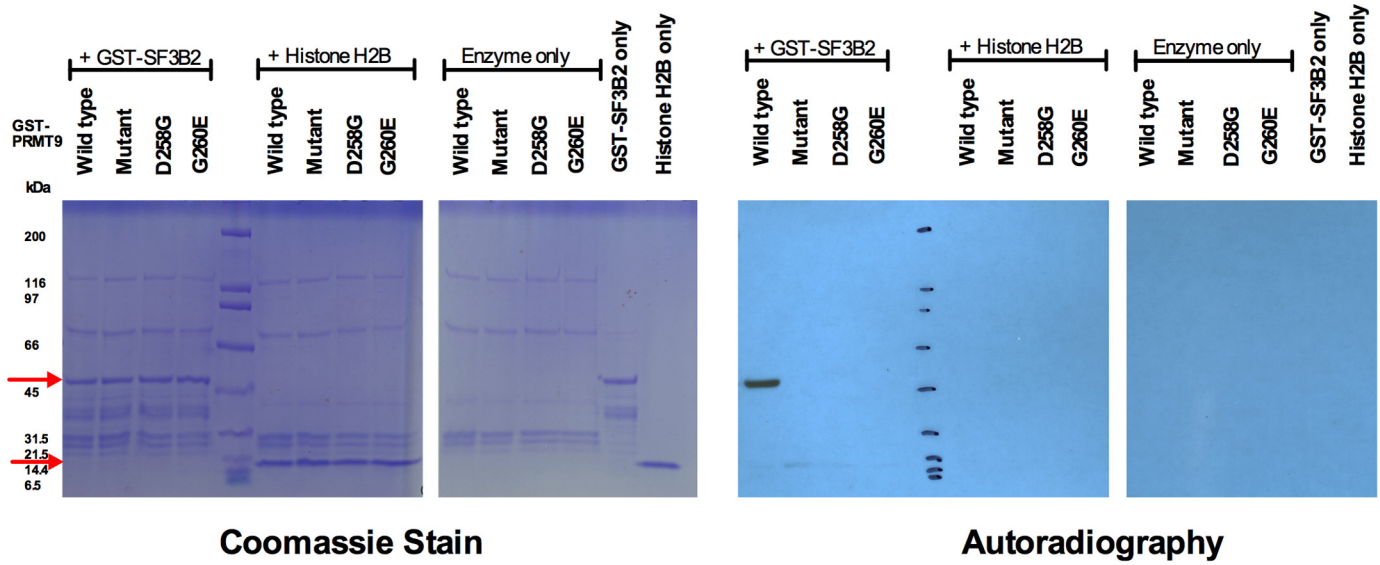

FIGURE 7. **Importance of a single acidic residue in the double E loop of PRMT9.** Site-directed mutagenesis was utilized to mutate the important residues mentioned in Fig. 6. Asp-258 was mutated to Gly to mimic type I enzymes, and Gly-260 was mutated to Glu to mimic PRMT7. The mutants were sequenced on both strands to confirm the mutation and bacterially expressed and purified as described under "Experimental Procedures." Methylation reactions were prepared using two PRMT substrates, PRMT9 substrate GST-SF3B2 401–550-residue wild type fragment (5 μg) purified as described under "Experimental Procedures" and PRMT7 protein substrate recombinant histone H2B (5 μg) purchased from New England Biolabs. Approximately 2 μg of enzyme (GST-PRMT9 wild type, catalytic mutant, D258G, or G260E) were added to the reaction with the indicated amount of substrate, along with 0.7 μM [*methyl*-^{3}H]AdoMet and methylation reaction buffer of 50 mM HEPES, 10 mM NaCl, 1 mM DTT, pH 8.0 at 37 °C for 1.5 h. Reactions were quenched by the addition of SDS loading buffer, run on 4–12% Bistris gel for SDS-PAGE, and dried as described under "Experimental Procedures." The dried gel was exposed to autoradiography film for 21 days at −80 °C. Molecular mass positions are indicated from 2 μg of unstained SDS-PAGE broad range markers (Bio-Rad, catalog no. 161-0317) electrophoresed in parallel lanes.

the corresponding residues, with both the position 4 Asp-147 and position 6 Glu-149 carboxyl groups also pointing away from the methylated arginine; this could account for the substrate specificity requirement of PRMT7 for an R*X*R motif (6). In addition, the crystal structure of human PRMT5 shows the position of the side chain of Phe-440, corresponding to Glu-149 in PRMT7 and Gly-260 in PRMT9, pointing away from the position of the methylated arginine (Fig. 6*D*) (39). These crystallographic and predicted structures led us to further probe these residues as being responsible for PRMT9's substrate specificity for the -FKRKY- sequence within the protein structure of SF3B2.

Site-directed Mutagenesis of Acidic Residue in PRMT9 Double E Loop Abolishes Recognition and Methylation of SF3B2—In probing for the residues responsible for PRMT9 substrate specificity, site-directed mutagenesis was done on residues in the double E loop described above and in Fig. 6. Asp-258 was mutated to Gly (D258G) to mimic type I enzymes, and Gly-260 was mutated to Glu (G260E) to mimic PRMT7. *In vitro* methylation reactions consisting of wild type, catalytic mutant, and mutants D258G and G260E were set up with GST-SF3B2 401–550-residue wild type fragment and recombinant histone H2B and analyzed by SDS-PAGE and autoradiography (Fig. 7). We found that PRMT9 lost all activity for SF3B2 when Asp-258 and Gly-260 were mutated, suggesting the importance of these residues in coordinating and binding of the substrate for methylation. *In vitro* methylation reactions with recombinant histone H2B, a good PRMT7 protein substrate due to its basic R*X*R sequences (6, 8), was also not recognized or methylated by either wild type enzyme or the D258G or G260E mutants. These results suggest that the local environment in the double E loop is crucial for catalysis.

Importance of PRMT9 Domains for Enzymatic Activity—Human PRMT9 contains three TPR motifs (residues 25–134) and two ancestrally duplicated methyltransferase domains (residues 135–530 and 531–895). This domain structure is unusual among the PRMT family, as no other PRMT contains a TPR motif, and only PRMT7 has a second methyltransferase domain. Several deletion constructs were made, in which the TPR motif was missing (ΔTPR), the N terminus was missing (ΔN; missing residues 21–350), and two C-terminal mutants ("ΔC 350," missing residues 351–895, and "ΔC 529," missing residues 530–895). These mutant enzymes were tested for enzymatic activity in *in vitro* methylation reactions by amino acid analysis (Fig. 8*A*). No activity was observed with any of the mutants after 16.5 h of incubation, a condition designed to detect any small amounts of product formation. Incubating the N- and C-terminal deletion constructs together did not result in enzyme activity (Fig. 8*A*). To rule out the possibility of degradation of the enzymes during the longer methylation reaction time, the reactions were set up in duplicate and incubated for 1 h, separated by SDS-PAGE, and subjected to autoradiography (Fig. 8*B*). Again, no activity was seen with the truncation mutants, suggesting that the intact, full-length PRMT9 protein is necessary for methylation activity.

Residues Surrounding the Arg-508 Methylation Site and the Position of the Methylated Arginine Are Important for Methyltransferase Activity—Because a synthetic peptide corresponding to the methylated region on SF3B2 could not be methylated by PRMT9 (Fig. 3*D*), the GST-SF3B2 401–550-residue wild type fragment was mutated to probe for the importance of the residues surrounding the Arg-508 site (-FKRKY-) using the more active GFP-PRMT9 enzyme (Fig. 9). The two flanking Lys residues were mutated to either Ala or Arg (Fig. 9, *B* and *C*). The

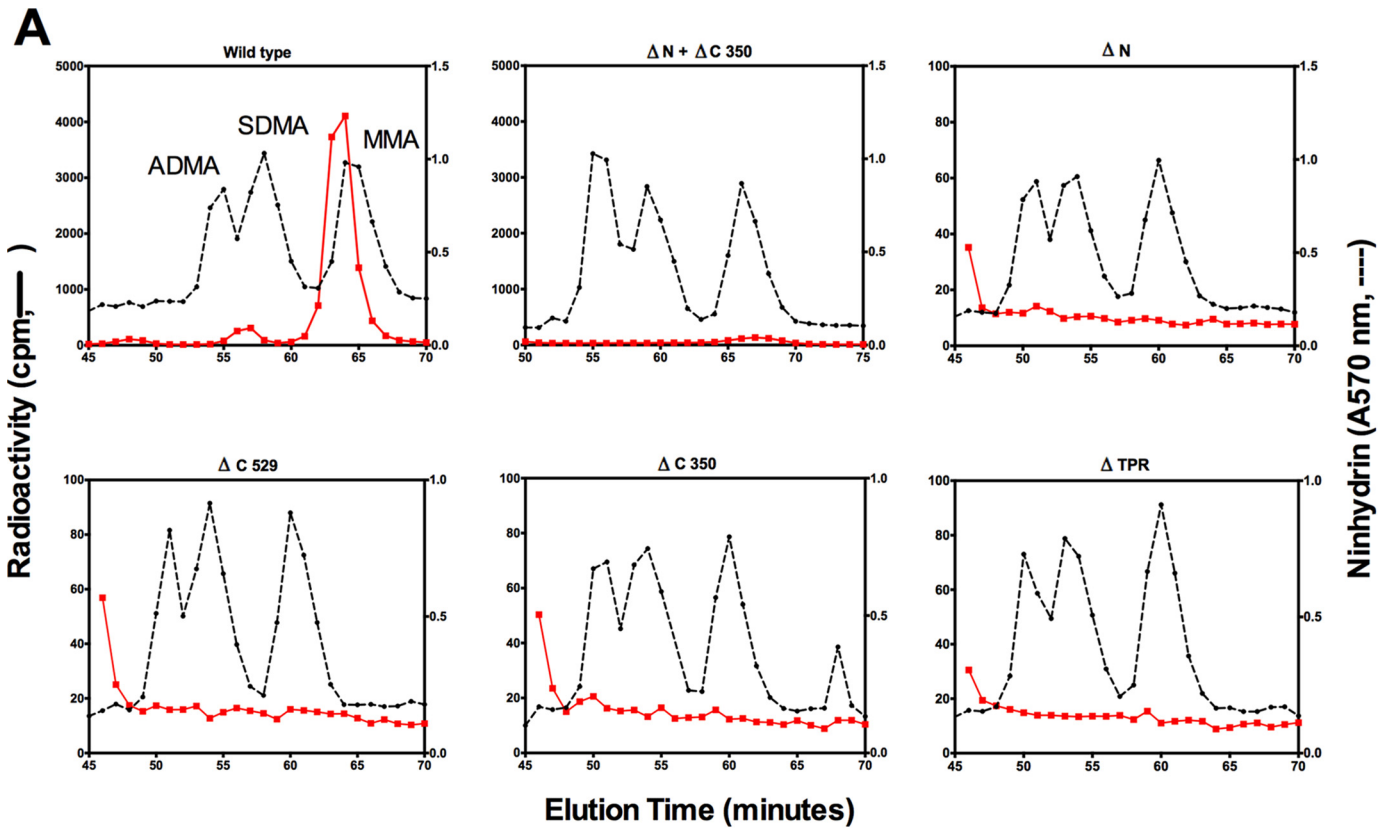
A
Wild type
ΔN + ΔC 350
ΔN
ΔC 529
ΔC 350
ΔTPR
ADMA
SDMA
MMA
Radioactivity (cpm, —)
Ninhydrin (A570 nm, ----)
Elution Time (minutes)

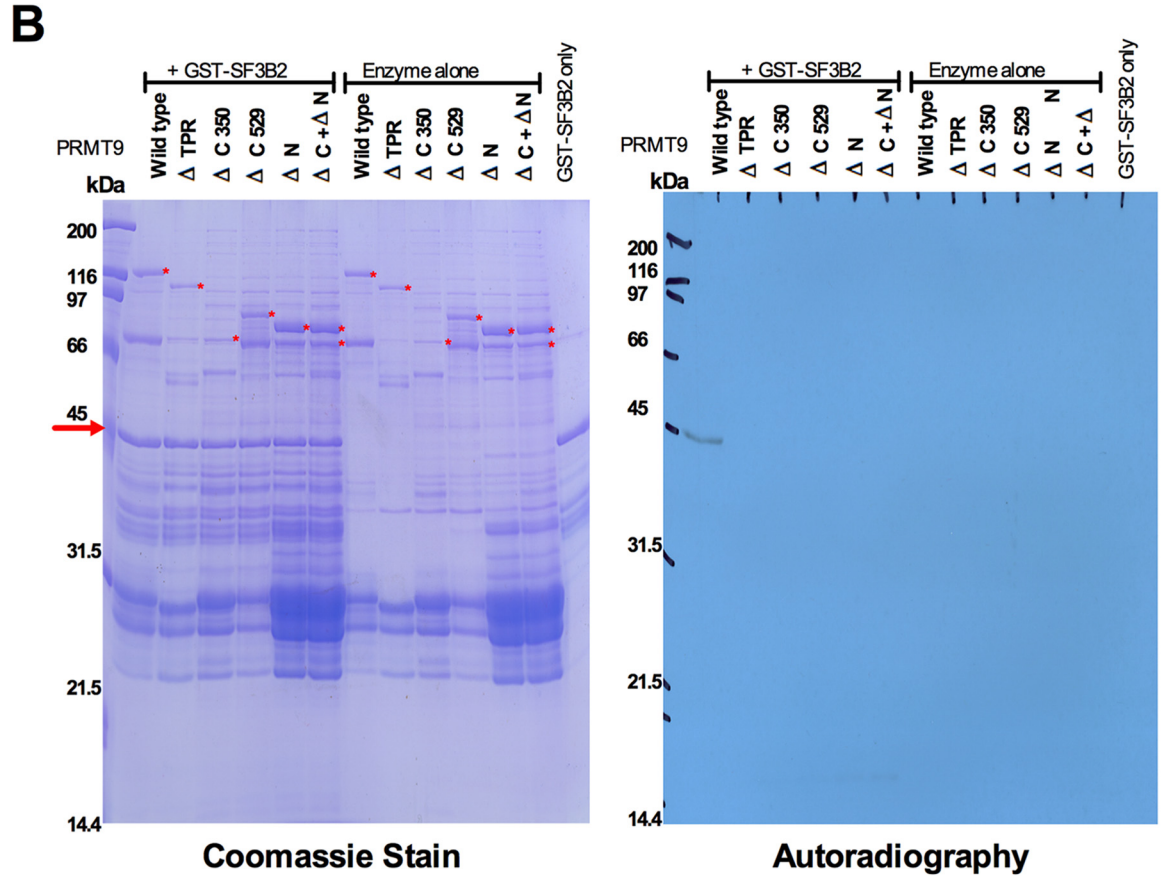
B
+ GST-SF3B2
Enzyme alone
PRMT9
kDa
Wild type
ΔTPR
ΔC 350
ΔC 529
ΔN
ΔC+ΔN
GST-SF3B2 only
200
116
97
66
45
31.5
21.5
14.4
Coomassie Stain
Autoradiography

-FARAY- and the -FRRRY- mutant proteins were both substrates for PRMT9 with moderately diminished formation of MMA but a greatly reduced formation of SDMA (Fig. 9, *B* and *C*). We next probed for the importance of the position of the methylatable arginine residue in the -FKRKY- sequence by moving its position upstream or downstream by one residue. An -FRKRY- protein was generated with the lysine and arginine residues switched, which resulted in an ~200-fold loss of MMA production and the complete loss of SDMA production (Fig. 9*D*). When only one arginine residue was present at the −1 position (-FRKKY-), we detected less than 0.3% of the activity with the wild type -FKRKY- sequence (Fig. 9*E*). These results suggest the importance of the position of the methylated arginine residue in the protein. In additional experiments, we mutated the two aromatic residues Phe-506 and Tyr-510 to Ala to look at the importance of π stacking or aromaticity in the binding of the substrate. Interestingly, the mutant construct -AKRKA- had a similar methyl-accepting activity as the wild type -FKRKY- protein (Fig. 9*A*). To confirm these results, we analyzed the polypeptides methylated after SDS-PAGE and autoradiography using the bacterially expressed GST-tagged PRMT9 enzyme (Fig. 9*G*). No methylation was observed with the GST-SF3B2 fragment protein in the mutants where the arginine residue was moved, although full activity was seen in the -AKRKA- mutant and partial activity in the -FARAY- and -FRRRY- proteins, consistent with the results obtained in Fig. 9, *A–F,* by amino acid analysis with the GFP-tagged enzyme.

Relative Contribution of the Type II PRMTs (5 and 9) in Mouse Embryo Fibroblasts—PRMT5 and PRMT9 are the only type II SDMA-forming enzymes known in mammals. We were thus interested in the relative roles of these two enzymes in total SDMA production. Using mouse embryo fibroblasts constructed so that PRMT5 expression could be turned off by induction with OHT, we analyzed proteins by immunoblotting with anti-PRMT5, anti-SDMA, anti-MMA, anti-ADMA, and anti-actin antibodies (Fig. 10*A*). We were able to reduce the PRMT5 protein to undetectable levels. There was little or no change in immunoreactivity to antibodies against ADMA and some loss of reactivity to antibodies against MMA. However, we found almost all of the immunoreactivity to the anti-SDMA BL8243 antibody, and most of that to the anti-SDMA BL8244 antibody, was lost in cells lacking PRMT5 (Fig. 10*A*). Significantly, an immunoreactive band with the anti-SDMA BL8244 antibody was seen at 145 kDa, which corresponds to the full-length form of the SF3B2 protein. This band is still present when PRMT5 is lost, suggesting it represents a product of PRMT9. Interestingly, there are also other bands that are immunoreactive with the anti-SDMA BL8244 antibody when PRMT5 is lost, particularly a major band found at 30 kDa in addition to other minor bands, which may indicate there are other cellular PRMT9 substrates that have yet to be discovered.

We also analyzed the total content of SDMA, ADMA, and MMA in these cells by quantitating fluorescent OPA amino acid derivatives after acid hydrolysis (Fig. 10, *B* and *C*). Wild type and PRMT5 knock-out lysates were acid-hydrolyzed and separated using cation exchange chromatography and then further derivatized using OPA. Analysis of the wild type sample shows the presence of ADMA and SDMA peaks after derivatization (Fig 10*B*, *top left panel*). Quantification of MMA and arginine levels were also done; arginine levels were used to normalize the content of MMA, SDMA, and ADMA (Fig 10, *B*, *top right panel,* and *C*) (29). When this analysis was repeated for the PRMT5-deficient cells, SDMA was not detected, although the levels of MMA and ADMA were similar to those of wild type cells (Fig. 10, *B*, *lower panels,* and *C*). These results indicate that the bulk of SDMA formation in mouse embryo fibroblasts is catalyzed by PRMT5 and that PRMT9 is responsible for only a small percentage of SDMA production.

Methylation of Splicing Factor SF3B2 and Myelin Basic Protein by PRMT9 and PRMT5—Finally, we wanted to determine how much cross-reactivity there may be between PRMT9 and PRMT5 with their major substrates SF3B2 and myelin basic protein, respectively. We incubated these enzymes with each of the substrates and [*methyl*-^{3}H]AdoMet under conditions to ensure that methylation was in the linear range and detected SDMA and MMA formation by amino acid analysis (Fig. 11). We found PRMT5 formed over 10 times more SDMA product with myelin basic protein than with SF3B2 (Fig 11, *A* and *B*). Under the same conditions, however, PRMT9 formed 40 times more SDMA with the SF3B2 401–550-residue wild type fragment as a substrate compared with myelin basic protein (Fig. 11, *C* and *D*). These results, combined with those shown in Fig. 10, indicate that PRMT5 and PRMT9 are unlikely to play redundant roles in the cell. The lethality of PRMT5 mouse knock-outs and a definite role of PRMT5 in embryonic development further support the nonredundant functions of these enzymes (3, 40, 41).

Discussion

We have shown that mammalian-expressed and bacterially expressed human PRMT9 have a protein arginine methyltransferase activity, joining PRMT5 as the second type II SDMA-forming enzyme in the mammalian PRMT family. Our previous work had identified the enzyme and its substrate, splicing factor SF3B2, and also provided evidence for a biological role as a modulator of splicing (7). In this work,

FIGURE 8. **Full-length intact enzyme is required for methyltransferase activity.** *A,* amino acid analysis of methylation reactions using GST-tagged PRMT9 truncation mutants with GST-SF3B2 401–550-residue wild type fragment. Approximately 2 μg of each wild type and truncated enzyme was used in a 60-μl methylation reaction with 5 μg of GST-SF3B2 401–550-residue wild type fragment, 0.7 μM [*methyl*-^{3}H]AdoMet, and methylation reaction buffer of 50 mM HEPES, 10 mM NaCl, 1 mM DTT, pH 8.0, at 37 °C for 16.5 h. Acid hydrolysis and amino acid analysis was carried out as described under "Experimental Procedures." *B,* autoradiography of ^{3}H-methylated GST-SF3B2 wild type fragment after reaction with wild type or truncation mutant GST-PRMT9 enzymes. Reactions were set up as described in *A* but were run for only 1 h to prevent possible degradation of the enzymes. Reactions were quenched and run on SDS-PAGE as described under "Experimental Procedures." Dried gels were exposed to film for 3 days at −80 °C and run in experimental triplicates on separate gels, one of which is shown here. Molecular mass positions are indicated from 2 μg of unstained SDS-PAGE broad range markers (Bio-Rad, catalog no. 161-0317) electrophoresed in parallel lanes.

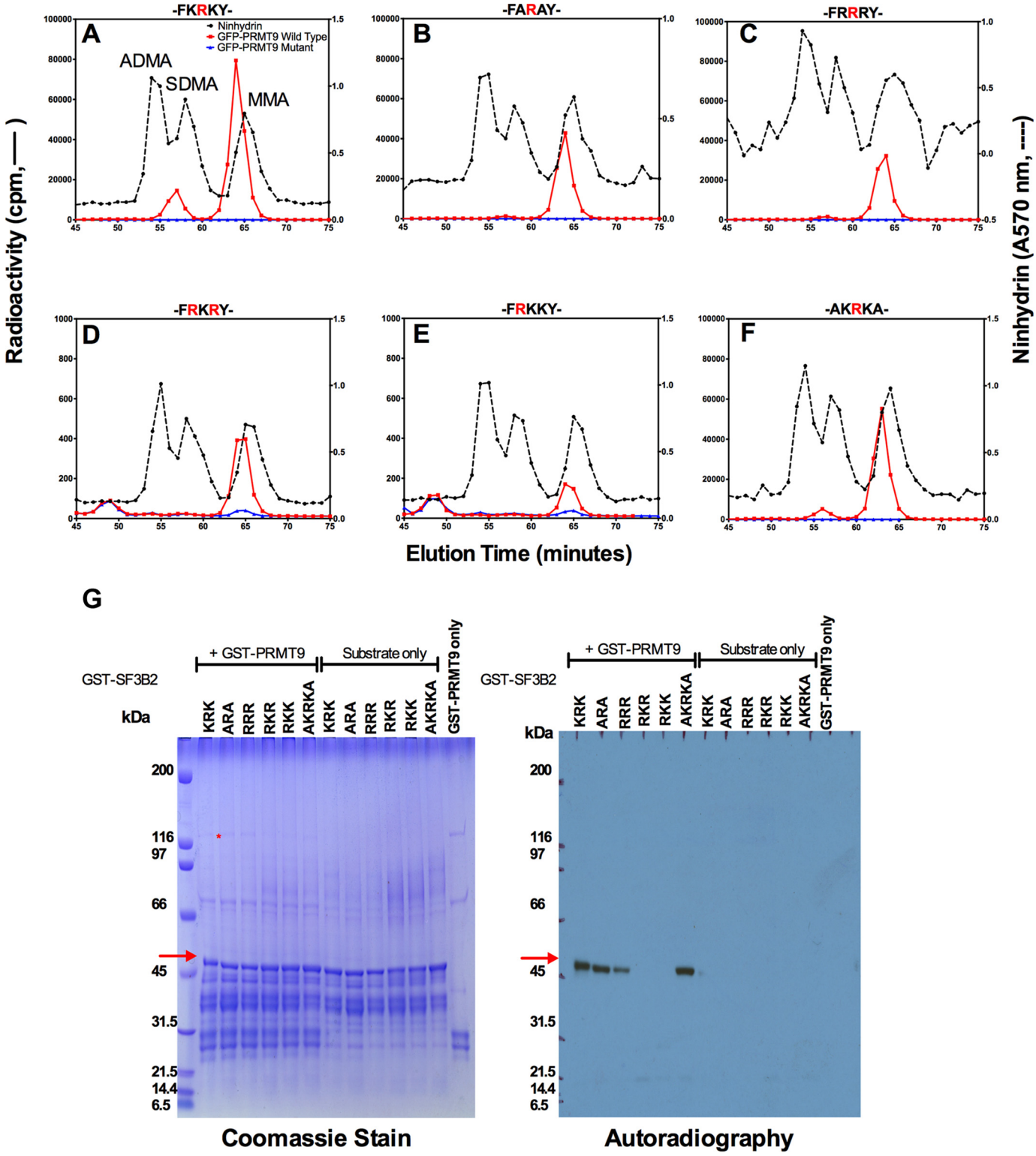

FIGURE 9. **Amino acids surrounding the Arg-508 site are important for substrate recognition and methylation.** *A–F*, point mutants were generated on the GST-SF3B2 401–550-residue wild type fragment where amino acids surrounding the Arg-508 methylation site were changed; mutants include K507A/K509A (-FARAY-), K507R/K509R (-FRRRY-), K507R/R508K/K509R (-FRKRY-), K507R/R508K (-FRKKY-), and F506A/Y510A (-AKRKA-). Methylation reactions were set up using mammalian-expressed wild type and catalytic mutant GFP-PRMT9 enzymes (1 μg) and GST-SF3B2 wild type or mutant fragments (5 μg), along with 0.7 μM [*methyl*-^{3}H]AdoMet, and methylation reaction buffer of 50 mM HEPES, 10 mM NaCl, 1 mM DTT, pH 8.0 at 37 °C for 16.5 h. Acid hydrolysis and amino acid analysis was carried out as described above under "Experimental Procedures." *G*, autoradiography of ^{3}H-methylated GST-SF3B2 401–550-residue wild type and mutant fragments (5 μg) with GST-PRMT9 wild type enzyme (2 μg) after a 16.5-h reaction. Reactions were set up with the same conditions as described in *A*. Reactions were quenched by addition of SDS-loading buffer, run on gels, and prepared for autoradiography as described under "Experimental Procedures." Dried gels were exposed to film for 3 days at −80 °C and run as experimental duplicates on separate gels, one of which is shown here. Molecular mass positions are indicated from 2 μg of unstained SDS-PAGE broad range markers (Bio-Rad, catalog no. 161-l0317) electrophoresed in parallel lanes.

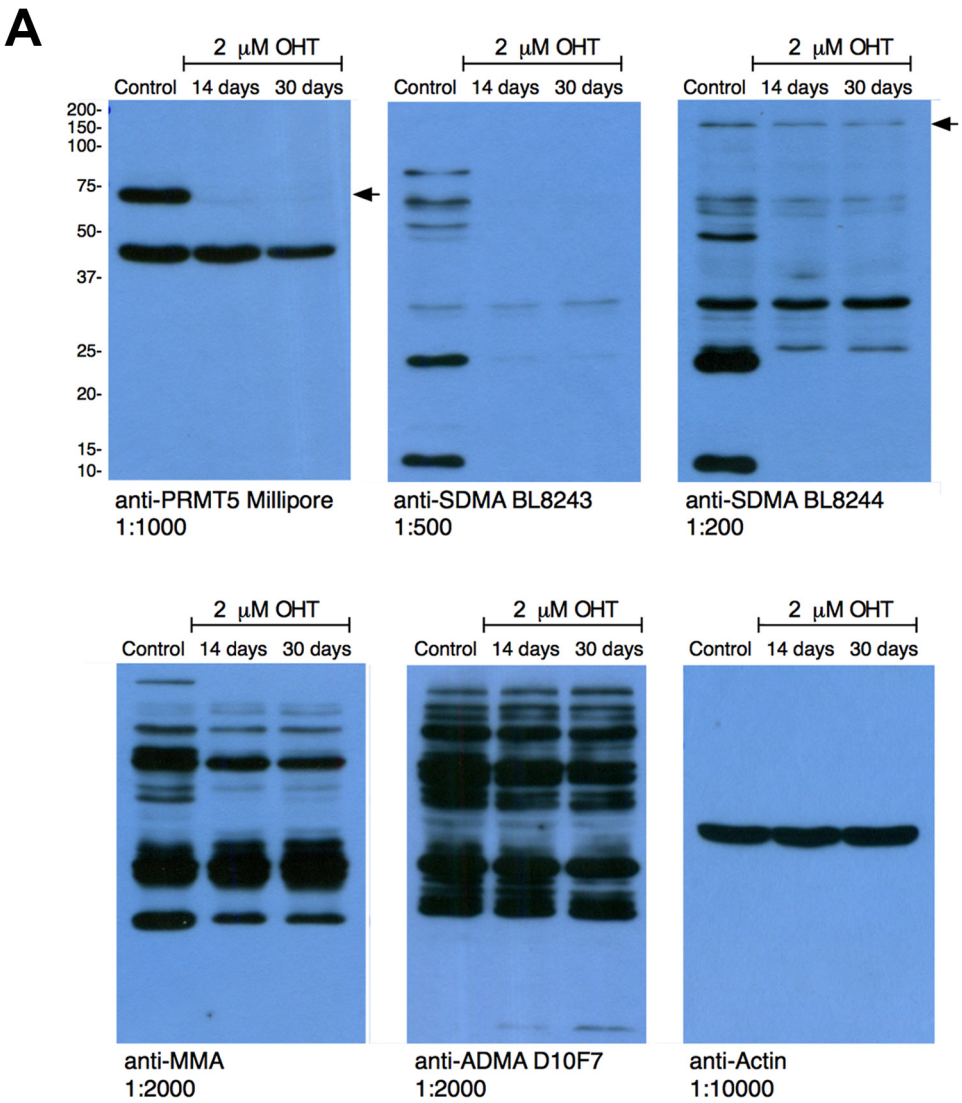

FIGURE 10. **Quantification of SDMA levels in protein hydrolysates of wild type and PRMT5 knock-out MEFs.** *A,* immunoblot showing wild type and PRMT5 knock-out MEFs treated for 14 and 30 days with 2 μM OHT. Whole cell lysates were prepared, run on SDS-PAGE, and immunoblotted using a panel of antibodies. Anti-PRMT5 (Millipore) antibody was used at a 1:1000 dilution to ensure efficient knockdown of PRMT5 in the OHT-treated cells. Anti-SDMA BL8243 and BL8244 were used at 1:500 and 1:200 dilution, respectively, to probe for cellular SDMA levels after PRMT5 knock-out. Anti-MMA (1:2000 dilution) and anti-ADMA D10F7 (1:2000 dilution) antibodies were also used to monitor cellular MMA and ADMA levels in wild type *versus* PRMT5 knock-out samples. Anti-actin (1:10,000 dilution) antibody was used to ensure equal loading. *B,* wild type and PRMT5 knock-out MEFs were harvested (40 mg), and the cell pellet was acid-hydrolyzed and run on amino acid analysis as described above under "Experimental Procedures," except no exogenous methylarginine standards were added to the samples. The resulting fractions from the amino acid analysis were derivatized using OPA for fluorescence quantification using reverse phase HPLC as described under "Experimental Procedures." Raw chromatographs show fluorescence at 455 nm, with peaks corresponding to individual fractions from the amino acid analysis that matched the elution of each methylated derivative (wild type, *top left*, PRMT5 knock-out, *bottom left*). Area comparison (wild type, *top right*; PRMT5 knock-out, *bottom right*) is shown as a quantification of the area under the peak for individual fractions from the amino acid analysis, using the raw data for ADMA (*red line*) and SDMA (*blue line*) peaks shown in the *left panels* and also quantifying MMA (*black dotted line*) amounts (raw chromatograms for MMA not shown). *C,* ratios of methylated arginine species/arginine. Quantification of arginine was used as an internal control for loading and easier comparison across sample replicates. To determine total area, the area under the raw chromatograph peaks (shown in *B*, *left* and *right panels*) was summed for each modification (ADMA, SDMA, and MMA) and corrected for dilution factors in preparation of the sample for OPA analysis. Total areas for each methylarginine species were then compared with the sum of the total area under the raw chromatographs for arginine, to give a ratio of modification/arginine. Data were gathered in experimental duplicate shown as the mean, and *bars* indicate the range of the data.

we have biochemically characterized the residues important for the PRMT9/SF3B2 enzyme-substrate interaction.

PRMT9 is an unusual protein arginine methyltransferase, as it has rather strict substrate specificity, an intact protein requirement for methylation, and contains a second methyltransferase domain and an additional acidic residue in its substrate-binding motif similar to human PRMT7. Its known substrate and binding partner in the cell, SF3B2, contains a methylatable sequence WCFKRKYLQ, which is not found in other proteins. Other proteins have similar sequences when -FKRKY- is searched, but no other proteins contain this extended sequence. PRMT9 has little or no activity on common PRMT substrates such as GST-GAR, myelin basic protein, or histones, suggesting an explicit role in splicing. We have shown that PRMT9 does not methylate a peptide with the WCFKRKYLQ sequence from SF3B2, suggesting that the substrate protein must be intact to make the correct contacts with the enzyme. In addition, we have demonstrated that N- and

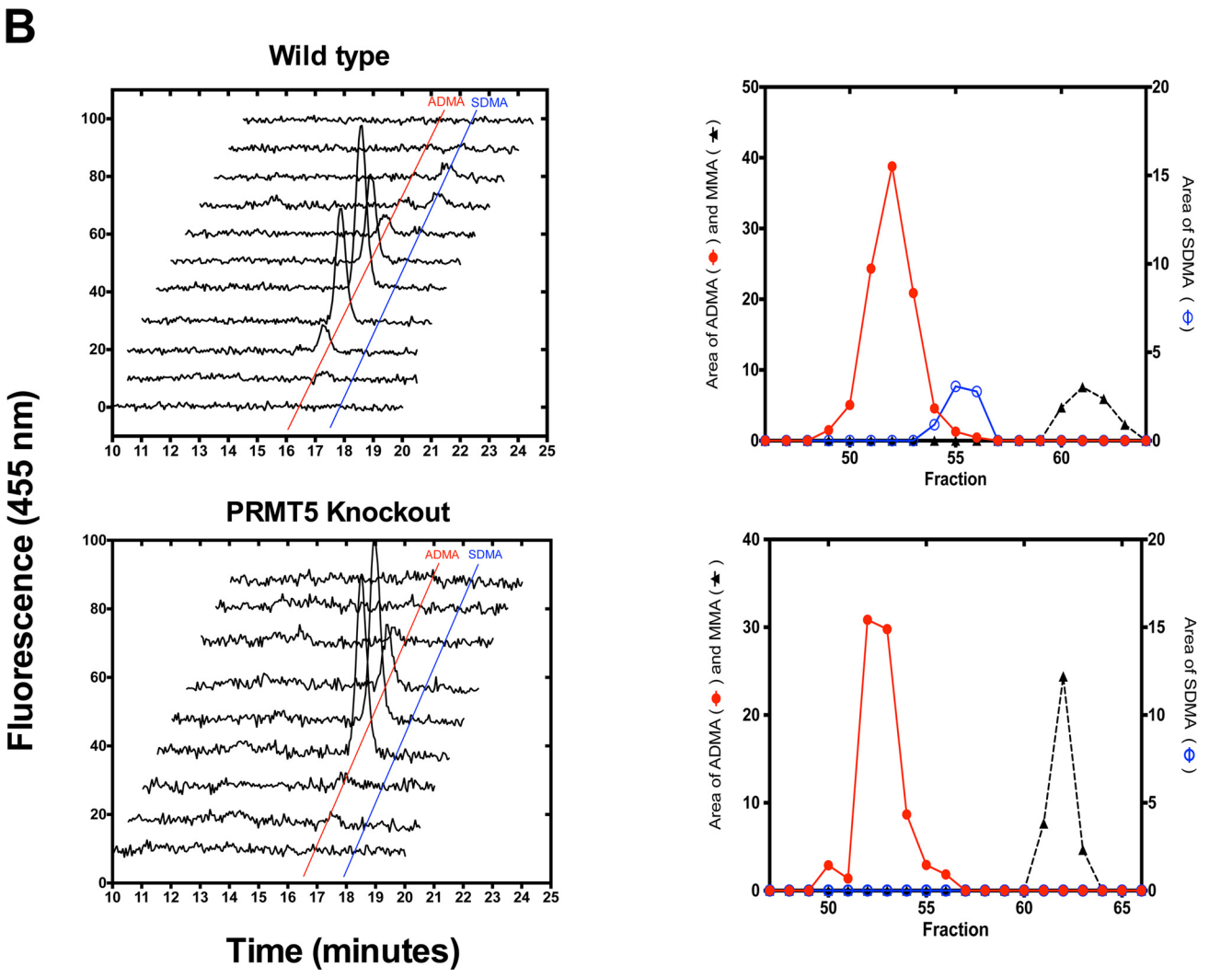

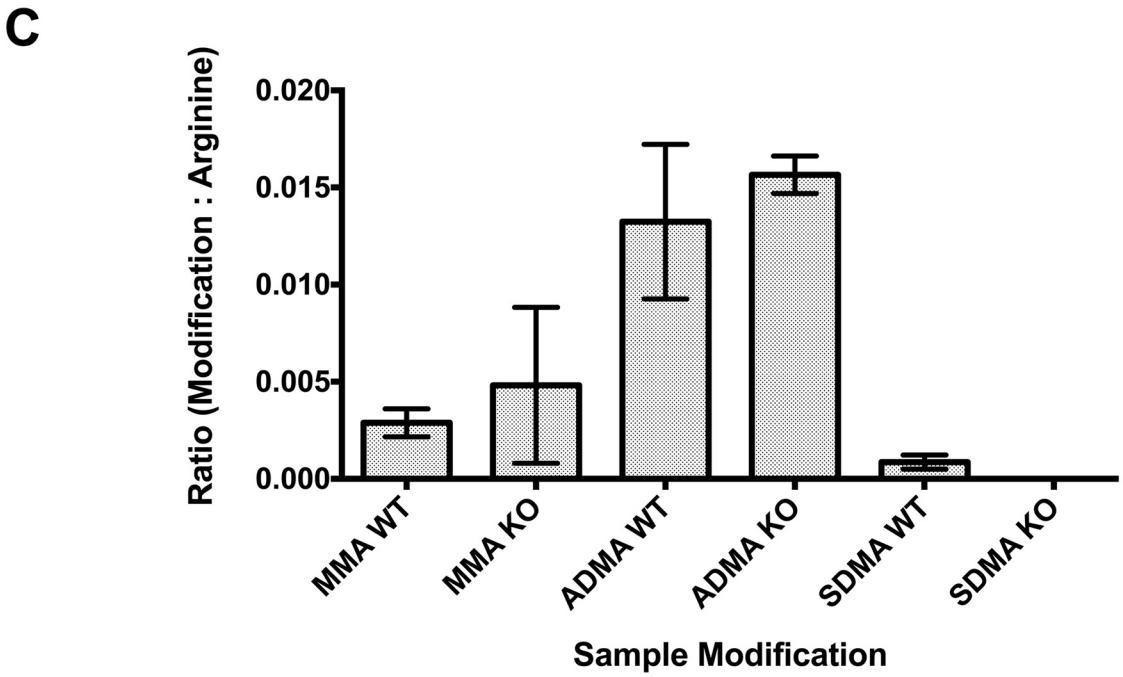

FIGURE 10—***Continued***

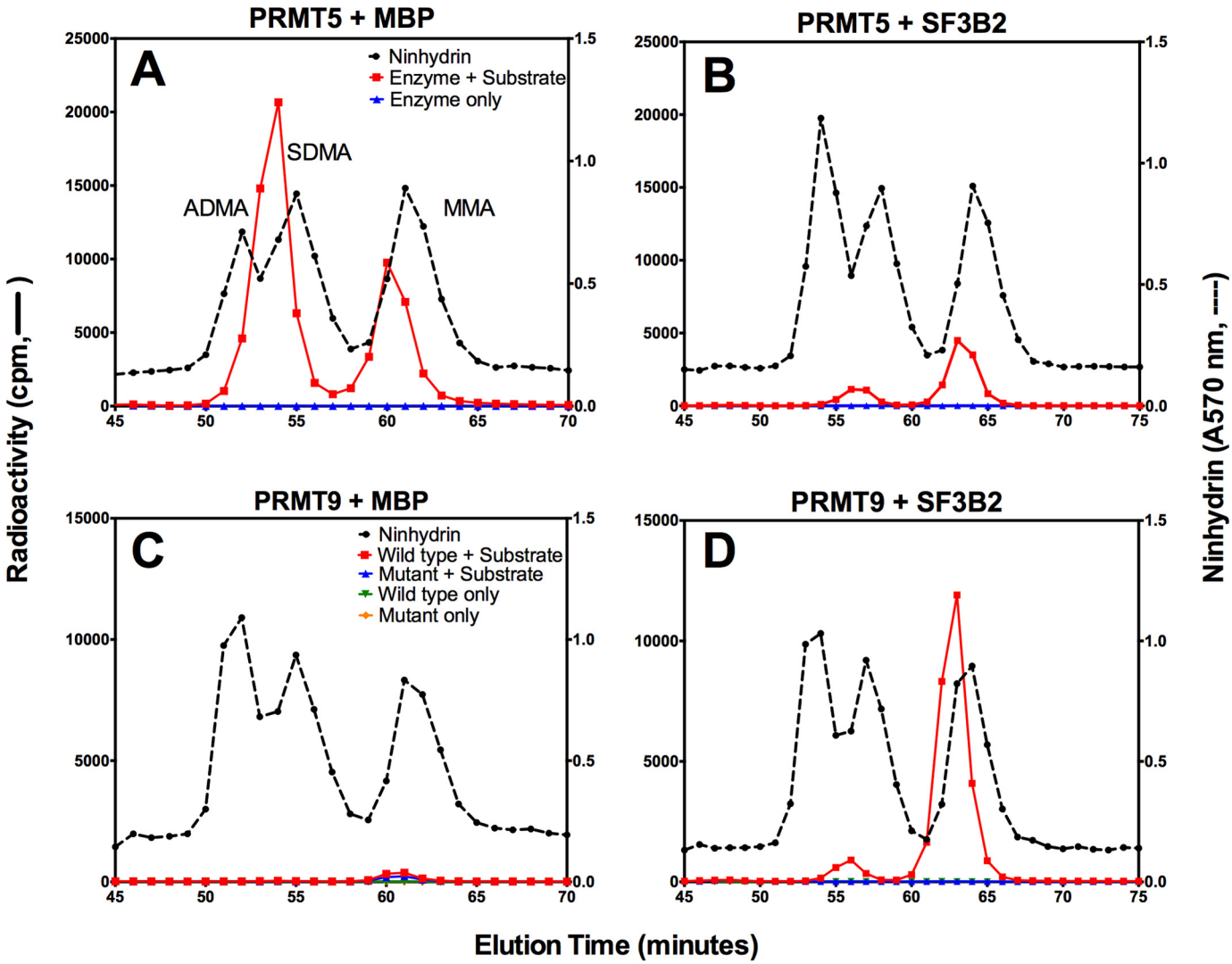

FIGURE 11. **PRMT5 and PRMT9 substrates are nonredundant.** *A,* amino acid analysis of PRMT5 (2.3 μg) and human His-tagged MBP (5 μg) after a 1-h *in vitro* methylation reaction, with 0.7 μM [*methyl*-^{3}H]AdoMet, and methylation reaction buffer of 25 mM Tris, 1 mM DTT, 8% glycerol, pH 8.0, at 37 °C in a 60-μl reaction volume. Acid hydrolysis and amino acid analysis was carried out as described under "Experimental Procedures." The *dotted black line* indicates ninhydrin absorbance at 570 nm for the nonradiolabeled methylated amino acid standards. The *red line* indicates the elution of the radioactive methylated amino acids of the wild type PRMT5 enzyme in reaction with the substrate. The *blue line* indicates the enzyme only control, to account for any background radioactivity. *B,* amino acid analysis of PRMT5 (2.3 μg) and GST-SF3B2 401–550-residue wild type fragment (5 μg) after a 1-h reaction, using same the conditions as described in *A*. *C,* amino acid analysis of *in vitro* methylation reaction of GFP-PRMT9 (wild type and catalytic mutant, 1 μg) with human His-tagged MBP (5 μg), with 0.7 μM [*methyl*-^{3}H]AdoMet, and methylation reaction buffer of 50 mM HEPES, 10 mM NaCl, 1 mM DTT, pH 8.0, at 37 °C in a 60-μl reaction volume. The *dotted black line* indicates the elution and ninhydrin absorbance at 570 nm for the nonradiolabeled methylated amino acids. The *red* and *blue lines* indicate the elution of the radioactive methylated amino acids of the substrate reacted with the wild type or catalytic mutant GFP-PRMT9, respectively. The *green* and *orange lines* indicate the wild type or catalytic mutant enzyme only controls. *D,* amino acid analysis of GFP-PRMT9 (wild type and catalytic mutant, 1 μg) with GST-SF3B2 401–550-residue wild type fragment (5 μg) after a 1-h reaction, using same conditions as described in *C*.

C-terminal deletions and TPR motif deletions of PRMT9 are inactive, further promoting the idea that the substrate must make correct contacts with both domains of the enzyme to be properly methylated. Structural studies have shown that PRMT1, PRMT3, and PRMT5 and *T. brucei* PRMT7 form homodimers in solution to methylate their substrates (15, 17–19), which may indicate that the second methyltransferase domain of PRMT9 functions to form a pseudodimer upon binding its substrate. Other studies have shown that substrates make important contacts on other parts of the enzyme, as is the case for PRMT1 with certain substrates (17), which would support our results. It should be noted, however, that PRMT1 and several other PRMTs like PRMT7, are also able to bind and methylate synthetic peptides (6, 8, 17, 39, 42).

Probing for the substrate residues important for methylation, we find that the position of the methylated arginine to be indispensable, possibly indicating a precise placement in the double E loop when AdoMet is bound (Fig. 6*B*). When the residues surrounding Arg-508 site are changed, SDMA is drastically reduced, and the amount of MMA formed is slightly affected. When the two lysines surrounding the target arginine are mutated to arginine, the presence of the extra positive charge in the active site seems to have detrimental effects, compared with when they are mutated to alanine. Furthermore, if the arginine residue is moved, we see almost completely abolished activity. Mutation of aromatic residues Phe-506 and Tyr-510 also seem to only slightly affect activity. This methylated sequence specificity is relatively uncommon, as the majority of PRMTs meth-

ylate RG-rich sequence motif (2, 3), with PRMT7 being the only other PRMT requiring a basic residue-rich environment for methylation (6, 8).

It is possible that the unique properties of PRMT9 within the PRMT family have been evolved to specifically recognize splicing factor SF3B2. In general, the phylogenetic distribution of PRMT9 and SF3B2 match each other (Fig. 1), although some organisms (higher plants) have the splicing factor but not PRMT9, and some organisms, such as chickens, have PRMT9 but not the splicing factor. It is also very interesting that although PRMT9 is found throughout the chordates, it is not widespread in invertebrates. For example, PRMT9 is clearly present in the sea anemone *N. vectensis* but is absent in the fruit fly *Drosophila melanogaster*. It is still unclear whether the *C. elegans prmt-3* gene encodes a PRMT9 ortholog. This protein, shown to methylate recombinant human histone H2A to form MMA only (31), has the conserved aspartate in position 4 of the double E loop but is more divergent than the chordate members of the PRMT9 family. No good orthologs of PRMT9 are found in plants, fungi, and other single cellular organisms. Novel BLAST-based methods have been developed to examine the evolutionary relationship between PRMTs in mammals and across various species, which provides insight into the evolutionary history of PRMTs (30, 43). Here, the closest relative of PRMT9 is PRMT7, with a close branch off of the PRMT5 outlier (30, 43). Interestingly, there is a wide evolutionary conservation of SF3B2 and the Arg-508 site across vertebrates, invertebrates, plants, fungi, and some unicellular organisms (Fig. 1, *C* and *D*). This may suggest that higher organisms found a need for regulation of splicing in the cell, and thus PRMT9 evolved or branched off from the rest of the PRMT family and PRMT7 to take on this function. Studies of orthologs of PRMT9 in other organisms would be of great interest, to determine whether the enzyme still has the same activity type, substrate specificity, and role in the cell. In addition, studying the relative distribution of the amounts of SDMA produced by PRMT9 compared with PRMT5 in other organisms would indicate an evolutionary relationship and need for regulation.

Tissue distribution studies show wide expression of PRMT9 in the body, with high protein expression in the testis, kidneys, skin, and hematopoietic and central nervous system (34, 44). PRMT9 has also been shown to have high expression in certain types of cancer, including lymphoma, melanoma, testicular, and pancreatic cancers (34). In addition, because of the involvement of SF3B2 in cell cycle progression and potential involvement in HIV hijacking/retroviral activity (14), it would be important to probe for the role of SF3B2 methylation in relation to viral and disease impact.

Although it does produce symmetrically dimethylated arginine, this enzyme is a minor contributor to the pool of SDMA in mouse embryo fibroblasts, compared with PRMT5 (Fig. 10). PRMT5 knock-out MEFs show no detectable SDMA by OPA analysis and greatly reduced SDMA by immunoblot analysis, indicating that PRMT9 SDMA methylation is likely restricted to a few substrates. Our OPA analysis results are consistent with similar studies quantifying relative amounts of these methylated arginine derivatives after the depletion of PRMT1 in cells (29). Furthermore, our results suggest that PRMT5 and PRMT9 do not appear to have redundant roles in cells, as they do not strongly methylate each other's substrates (Fig. 11). Immunoblots of PRMT5 knock-out MEF whole cell lysates with anti-SDMA antibodies show the presence of minor bands, which may indicate the presence of other possible substrates for PRMT9 in the cell. It will be interesting to characterize these possible substrates and identify other potential roles for PRMT9.

Acknowledgments—We thank Marco Bezzi and Ernesto Guccione (National University of Singapore) for providing primary Prmt5$^{F/F}$-ER-Cre MEFs. We also thank Jorge Torres, Xiaoyu Xia, and Ankur Gholkar (UCLA) for their advice and assistance with mammalian cell culture and immunofluorescence. We also thank the Margot Quinlan lab (UCLA) for their help with immunofluorescence studies and Douglas Juers (Whitman College, Washington) for the gift of the His-MBP plasmid. Alexander Patananan provided valuable advice and help with the OPA analysis as well as helpful comments on the manuscript. You Feng, Jonathan Lowenson, Kanishk Jain, Qais Al-Hadid, and Cecilia-Zurita Lopez provided helpful advice on the research and the manuscript.

References

1. Herrmann, F., Pably, P., Eckerich, C., Bedford, M. T., and Fackelmayer, F. O. (2009) Human protein arginine methyltransferases *in vivo*–distinct properties of eight canonical members of the PRMT family. *J. Cell Sci.* **122,** 667–677
2. Bedford, M. T., and Clarke, S. G. (2009) Protein arginine methylation in mammals: Who, what, and why. *Mol. Cell* **33,** 1–13
3. Yang, Y., and Bedford, M. T. (2013) Protein arginine methyltransferases and cancer. *Nat. Rev. Cancer* **13,** 37–50
4. Fuhrmann, J., Clancy, K. W., and Thompson, P. R. (2015) Chemical biology of protein arginine modifications in epigenetic regulation. *Chem. Rev.* 10.1021/acs.chemrev.5b00003
5. Lee, Y.-H., and Stallcup, M. R. (2009) Minireview: protein arginine methylation of nonhistone proteins in transcriptional regulation. *Mol. Endocrinol.* **23,** 425–433
6. Feng, Y., Maity, R., Whitelegge, J. P., Hadjikyriacou, A., Li, Z., Zurita-Lopez, C., Al-Hadid, Q., Clark, A. T., Bedford, M. T., Masson, J. Y., and Clarke, S. G. (2013) Mammalian protein arginine methyltransferase 7 (PRMT7) specifically targets RXR sites in lysine- and arginine-rich regions. *J. Biol. Chem.* **288,** 37010–37025
7. Yang, Y., Hadjikyriacou, A., Xia, Z., Gayatri, S., Kim, D., Zurita-Lopez, C., Kelly, R., Guo, A., Li, W., Clarke, S. G., and Bedford, M. T. (2015) PRMT9 is a Type II methyltransferase that methylates the splicing factor SAP145. *Nat. Commun.* 10.1038/ncomms7428
8. Feng, Y., Hadjikyriacou, A., and Clarke, S. G. (2014) Substrate specificity of human protein arginine methyltransferase 7 (PRMT7): the importance of acidic residues in the double E loop. *J. Biol. Chem.* **289,** 32604–32616
9. Molina-Serrano, D., Schiza, V., and Kirmizis, A. (2013) Cross-talk among epigenetic modifications: lessons from histone arginine methylation. *Biochem. Soc. Trans.* **41,** 751–759
10. Yoshimatsu, M., Toyokawa, G., Hayami, S., Unoki, M., Tsunoda, T., Field, H. I., Kelly, J. D., Neal, D. E., Maehara, Y., Ponder, B. A., Nakamura, Y., and Hamamoto, R. (2011) Dysregulation of PRMT1 and PRMT6, type I arginine methyltransferases, is involved in various types of human cancers. *Int. J. Cancer* **128,** 562–573
11. Baldwin, R. M., Morettin, A., and Côté, J. (2014) Role of PRMTs in cancer: Could minor isoforms be leaving a mark? *World J. Biol. Chem.* **5,** 115–129
12. Duan, S., Cermak, L., Pagan, J. K., Rossi, M., Martinengo, C., di Celle, P. F., Chapuy, B., Shipp, M., Chiarle, R., and Pagano, M. (2012) FBXO11 targets BCL6 for degradation and is inactivated in diffuse large B-cell lymphomas. *Nature* **481,** 90–93
13. Champion-Arnaud, P., and Reed, R. (1994) The prespliceosome compo-

nents SAP 49 and SAP 145 interact in a complex implicated in tethering U2 snRNP to the branch site. *Genes Dev.* **8,** 1974–1983
14. Terada, Y., and Yasuda, Y. (2006) Human immunodeficiency virus type 1 Vpr induces G2 checkpoint activation by interacting with the splicing factor SAP145. *Mol. Cell. Biol.* **26,** 8149–8158
15. Hasegawa, M., Toma-Fukai, S., Kim, J. D., Fukamizu, A., and Shimizu, T. (2014) Protein arginine methyltransferase 7 has a novel homodimer-like structure formed by tandem repeats. *FEBS Lett.* **588,** 1942–1948
16. Cura, V., Troffer-Charlier, N., Wurtz, J.-M., Bonnefond, L., and Cavarelli, J. (2014) Structural insight into arginine methylation by the mouse protein arginine methyltransferase 7: a zinc finger freezes the mimic of the dimeric state into a single active site. *Acta Crystallogr. D Biol. Crystallogr.* **70,** 2401–2412
17. Lee, D. Y., Ianculescu, I., Purcell, D., Zhang, X., Cheng, X., and Stallcup, M. R. (2007) Surface-scanning mutational analysis of protein arginine methyltransferase 1: roles of specific amino acids in methyltransferase substrate specificity, oligomerization, and coactivator function. *Mol. Endocrinol.* **21,** 1381–1393
18. Tang, J., Gary, J. D., Clarke, S., and Herschman, H. R. (1998) PRMT3, a type I protein arginine *N*-methyltransferase that differs from PRMT1 in its oligomerization, subcellular localization, substrate specificity, and regulation. *J. Biol. Chem.* **273,** 16935–16945
19. Lott, K., Zhu, L., Fisk, J. C., Tomasello, D. L., and Read, L. K. (2014) Functional interplay between protein arginine methyltransferases in *Trypanosoma brucei*. *Microbiol. Open* **3,** 595–609
20. Miranda, T. B., Miranda, M., Frankel, A., and Clarke, S. (2004) PRMT7 is a member of the protein arginine methyltransferase family with a distinct substrate specificity. *J. Biol. Chem.* **279,** 22902–22907
21. Blatch, G. L., and Lässle, M. (1999) The tetratricopeptide repeat: a structural motif mediating protein-protein interactions. *BioEssays* **21,** 932–939
22. Wang, M., Xu, R.-M., and Thompson, P. R. (2013) Substrate specificity, processivity, and kinetic mechanism of protein arginine methyltransferase 5. *Biochemistry* **52,** 5430–5440
23. Wang, M., Fuhrmann, J., and Thompson, P. R. (2014) Protein arginine methyltransferase 5 catalyzes substrate dimethylation in a distributive fashion. *Biochemistry* **53,** 7884–7892
24. Meister, G., Eggert, C., Bühler, D., Brahms, H., Kambach, C., and Fischer, U. (2001) Methylation of Sm proteins by a complex containing PRMT5 and the putative U snRNP assembly factor pICln. *Curr. Biol.* **11,** 1990–1994
25. Tamura, K., Stecher, G., Peterson, D., Filipski, A., and Kumar, S. (2013) MEGA6: Molecular evolutionary genetics analysis version 6.0. *Mol. Biol. Evol.* **30,** 2725–2729
26. McWilliam, H., Li, W., Uludag, M., Squizzato, S., Park, Y. M., Buso, N., Cowley, A. P., and Lopez, R. (2013) Analysis tool web services from the EMBL-EBI. *Nucleic Acids Res.* **41,** 597–600
27. Zurita-Lopez, C. I., Sandberg, T., Kelly, R., and Clarke, S. G. (2012) Human protein arginine methyltransferase 7 (PRMT7) is a Type III enzyme forming ω-N^G-monomethylated arginine residues. *J. Biol. Chem.* **287,** 7859–7870
28. Bezzi, M., Teo, S. X., Muller, J., Mok, W. C., Sahu, S. K., Vardy, L. A., Bonday, Z. Q., and Guccione, E. (2013) Regulation of constitutive and alternative splicing by PRMT5 reveals a role for Mdm4 pre-mRNA in sensing defects in the spliceosomal machinery. *Genes Dev.* **27,** 1903–1916
29. Dhar, S., Vemulapalli, V., Patananan, A. N., Huang, G., Di Lorenzo, A., Richard, S., Comb, M. J., Guo, A., Clarke, S. G., and Bedford, M. T. (2013) Loss of the major Type I arginine methyltransferase causes substrate scavenging by Type II and III enzymes. *Sci. Rep.* **3,** 1311. doi: 10.1038/srep01311
30. Wang, Y. C., Wang, J. D., Chen, C. H., Chen, Y. W., and Li, C. (2015) A novel BLAST-based relative distance (BBRD) method can effectively group members of protein arginine methyltransferases and suggest their evolutionary relationship. *Mol. Phylogenet. Evol.* **84,** 101–111
31. Takahashi, Y., Daitoku, H., Yokoyama, A., Nakayama, K., Kim, J.-D., and Fukamizu, A. (2011) The *C. elegans* PRMT-3 possesses a type III protein arginine methyltransferase activity. *J. Recept. Signal Transduct. Res.* **31,** 168–172
32. Branscombe, T. L., Frankel, A., Lee, J. H., Cook, J. R., Yang, Z., Pestka, S., and Clarke, S. (2001) PRMT5 (Janus kinase-binding protein 1) catalyzes the formation of symmetric dimethylarginine residues in proteins. *J. Biol. Chem.* **276,** 32971–32976
33. Shaw, G., Morse, S., Ararat, M., and Graham, F. L. (2002) Preferential transformation of human neuronal cells by human adenoviruses and the origin of HEK 293 cells. *FASEB J.* **16,** 869–871
34. Uhlén, M., Fagerberg, L., Hallström, B. M., Lindskog, C., Oksvold, P., Mardinoglu, A., Sivertsson, Å., Kampf, C., Sjöstedt, E., Asplund, A., Olsson, I., Edlund, K., Lundberg, E., Navani, S., Szigyarto, C. A., *et al.* (2015) Proteomics. Tissue-based map of the human proteome. *Science* **347,** 10.1126/science.1260419
35. Katz, J. E., Dlakić, M., and Clarke, S. (2003) Automated identification of putative methyltransferases from genomic open reading frames. *Mol. Cell. Proteomics* **2,** 525–540
36. Gary, J. D., and Clarke, S. G. (1998) RNA and protein interactions modulated by protein arginine methylation. *Prog. Nucleic Acids Res. Mol. Biol.* **61,** 65–131
37. Bachand, F. (2007) Protein arginine methyltransferases: from unicellular eukaryotes to humans. *Eukaryot. Cell* **6,** 889–898
38. Kelley, L. A., and Sternberg, M. J. (2009) Protein structure prediction on the web: a case study using the Phyre server. *Nat. Protoc.* **4,** 363–371
39. Antonysamy, S., Bonday, Z., Campbell, R. M., Doyle, B., Druzina, Z., Gheyi, T., Han, B., Jungheim, L. N., Qian, Y., Rauch, C., Russell, M., Sauder, J. M., Wasserman, S. R., Weichert, K., Willard, F. S., *et al.* S. (2012) Crystal structure of the human PRMT5: MEP50 complex. *Proc. Natl. Acad. Sci. U.S.A.* **109,** 17960–17965
40. Tee, W. W., Pardo, M., Theunissen, T. W., Yu, L., Choudhary, J. S., Hajkova, P., and Surani, M. A. (2010) Prmt5 is essential for early mouse development and acts in the cytoplasm to maintain ES cell pluripotency service Prmt5 is essential for early mouse development and acts in the cytoplasm to maintain ES cell pluripotency. *Genes Dev.* **24,** 2772–2777
41. Dacwag, C. S., Bedford, M. T., Sif, S., and Imbalzano, A. N. (2009) Distinct protein arginine methyltransferases promote ATP-dependent chromatin remodeling function at different stages of skeletal muscle differentiation. *Mol. Cell. Biol.* **29,** 1909–1921
42. Gui, S., Wooderchak-Donahue, W. L., Zang, T., Chen, D., Daly, M. P., Zhou, Z. S., and Hevel, J. M. (2013) Substrate-induced control of product formation by protein arginine methyltransferase 1. *Biochemistry* **52,** 199–209
43. Wang, Y. C., and Li, C. (2012) Evolutionarily conserved protein arginine methyltransferases in non-mammalian animal systems. *FEBS J.* **279,** 932–945
44. Petryszak, R., Burdett, T., Fiorelli, B., Fonseca, N. A., Gonzalez-Porta, M., Hastings, E., Huber, W., Jupp, S., Keays, M., Kryvych, N., McMurry, J., Marioni, J. C., Malone, J., Megy, K., Rustici, G., et al. (2014) Expression Atlas update–a database of gene and transcript expression from microarray- and sequencing-based functional genomics experiments. *Nucleic Acids Res.* **42,** D926–D932
45. Gottschling, H., and Freese, E. (1962) A tritium isotope effect on ion exchange chromatography. *Nature* **196,** 829–831